Physique de l'atmosphère et transport

COURS 2

TRANSPORT ET MELANGE

SPECATMO

B. Legras, legras@lmd.ens.fr, http://www.lmd.ens.fr/legras

Transport et mélange

I Introduction et exemples

II Eléments de théorie

III Reconstructions des champs de traceurs

IV Barrières de transport

V Diagrammmes traceur-traceur et lignes de mélange

V Un exemple de méthode semi-lagrangienne

Source de traceurs

Dispersion d'un panache volcanique

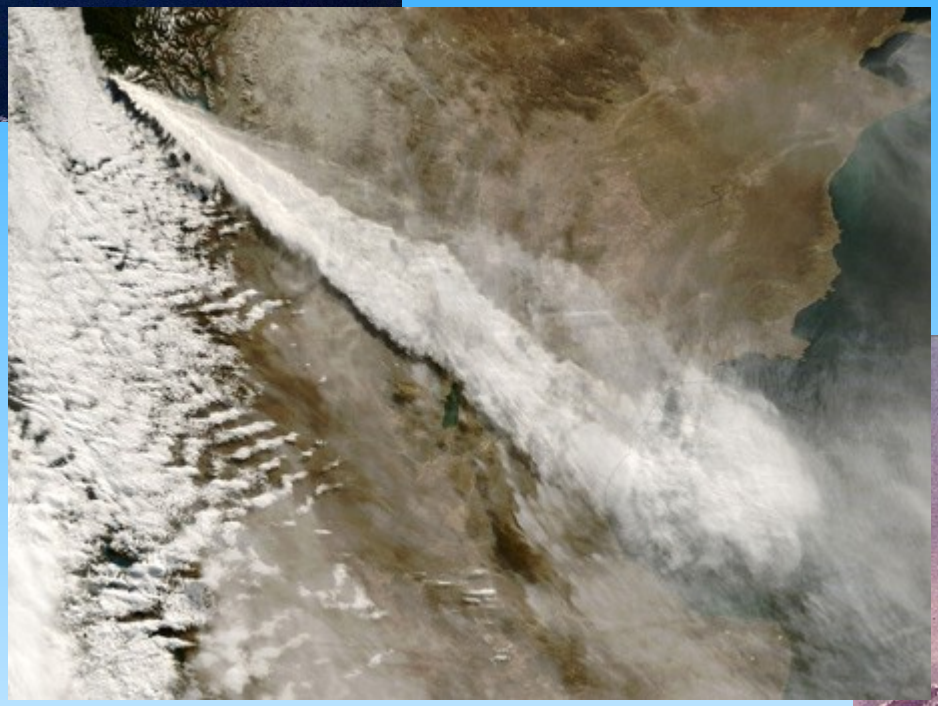

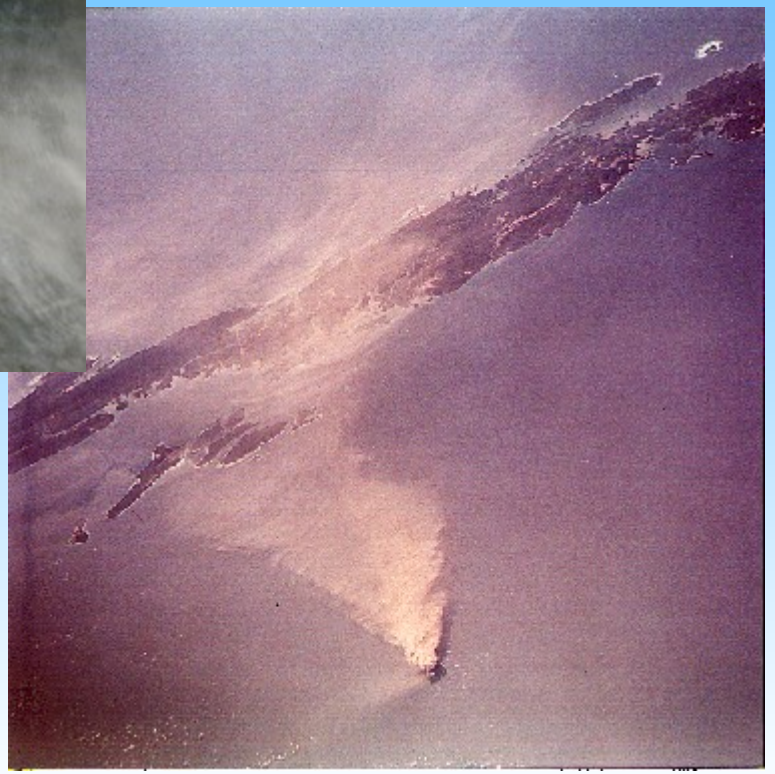

Remarquez:
- largeur croît en d ou plus rapidement à courte distance puis moins rapidement
- modulation par gros tourbillons

Feux agricoles à grande échelle en Afrique

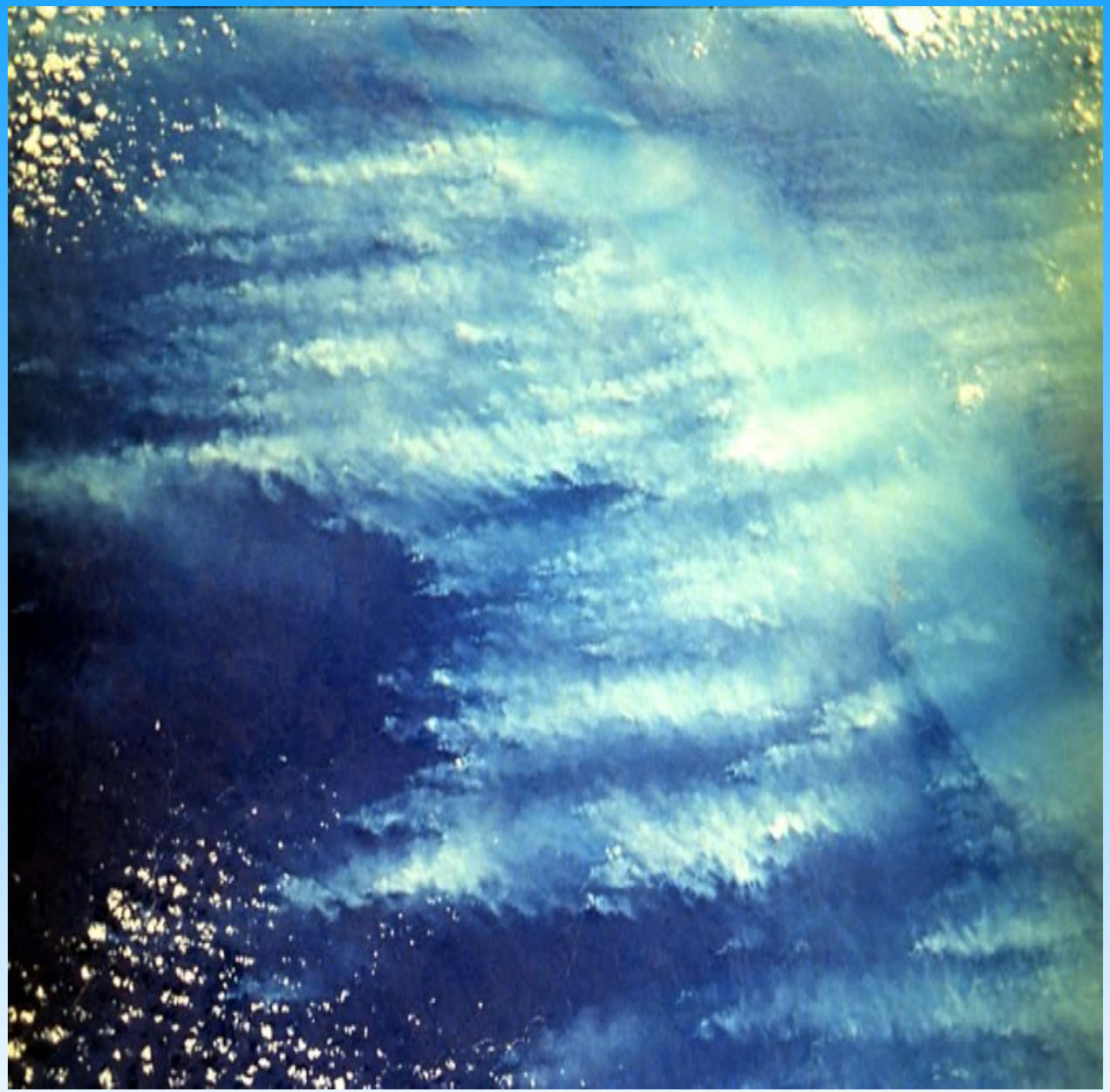

Chlorophyll in the ocean

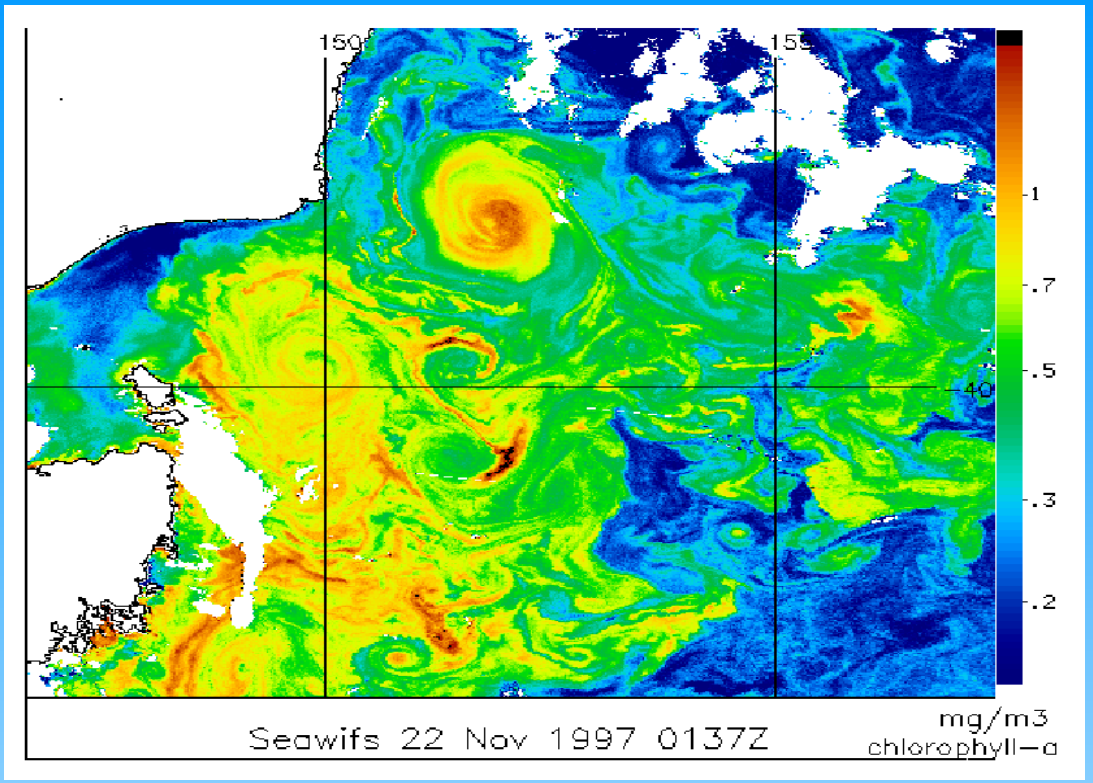

The distribution of long-live tracer depends to a large extend of transport and stirring by winds and oceanic currents.

Biological production in the ocean and chemical reactions in the atmosphere depend on mixing which is performed by the turbulent motion.

Huge Reynolds number $O(10^{10})$

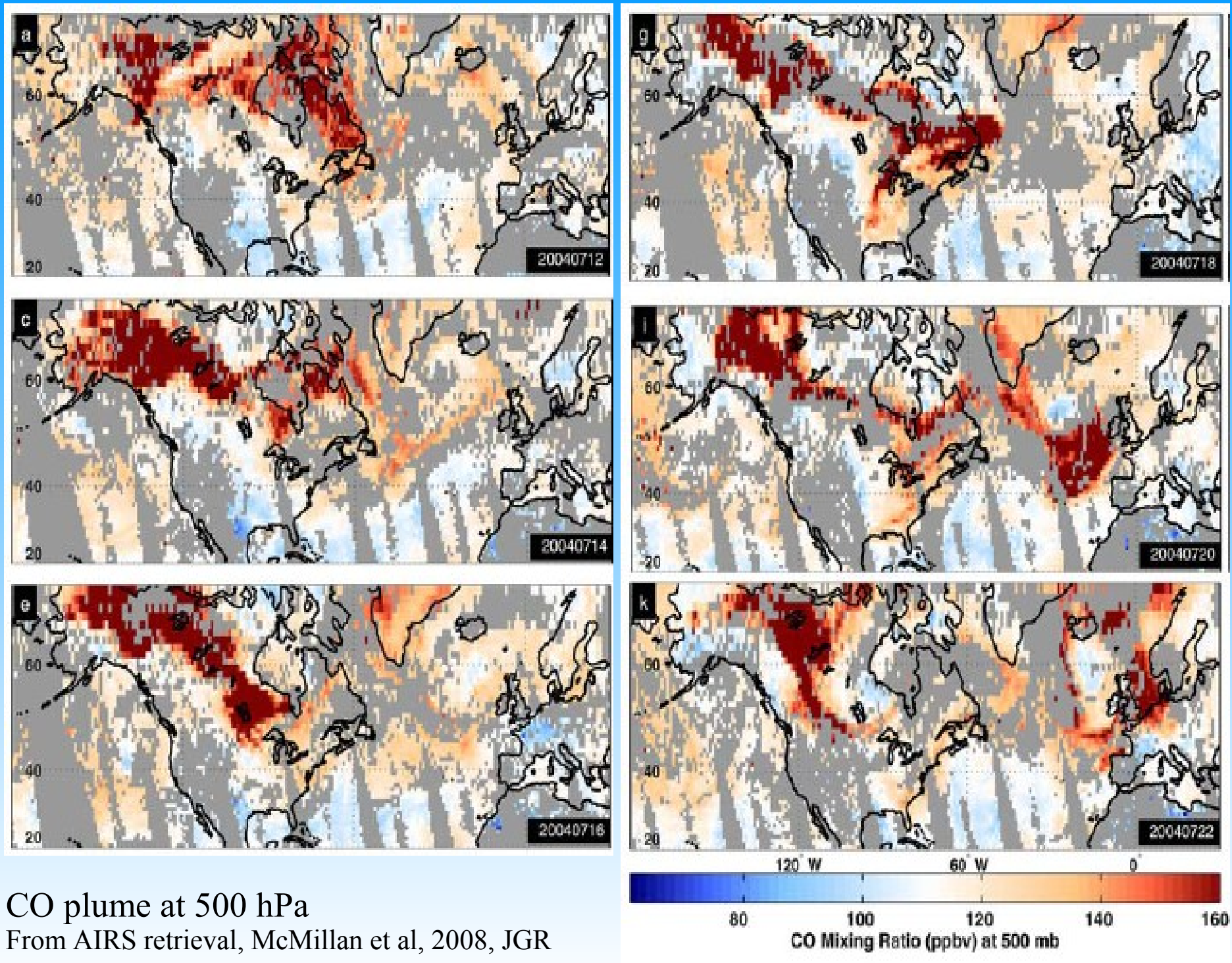

CO plume at 500 hPa

From AIRS retrieval, McMillan et al, 2008, JGR

Large-scale motion (L>100 km in the atmosphere, L>10 km in the ocean) is dominated by layerwise quasi two-dimensional motion as a result of aspect-ratio, rotation and stratification

Numerically simulated two-dimensional turbulence

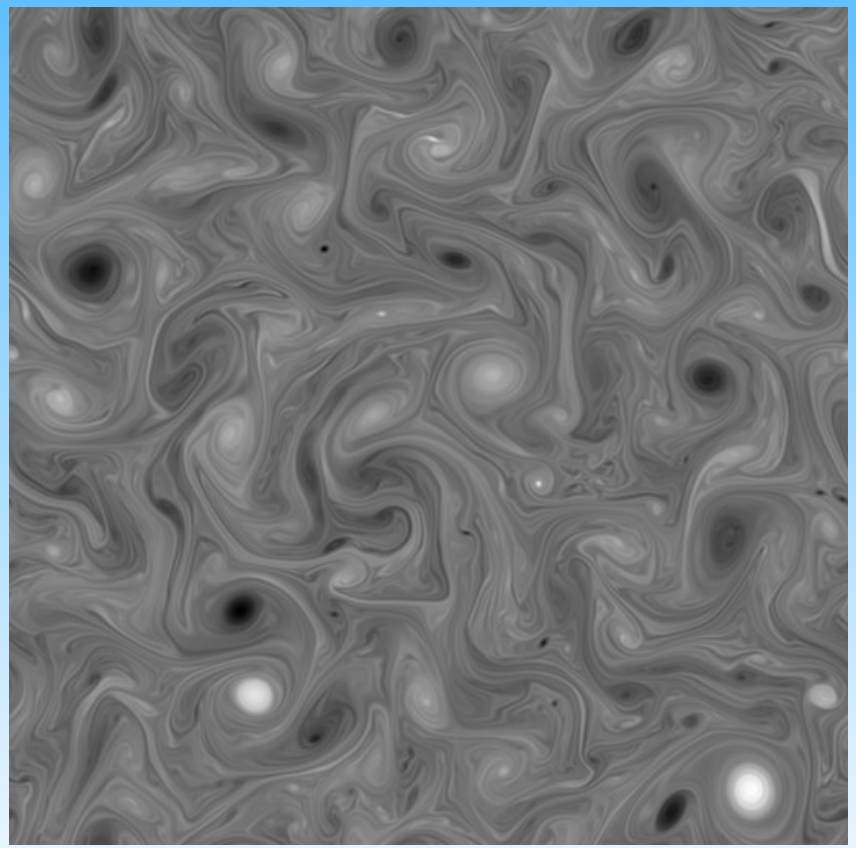

Chlorophyll in the ocean

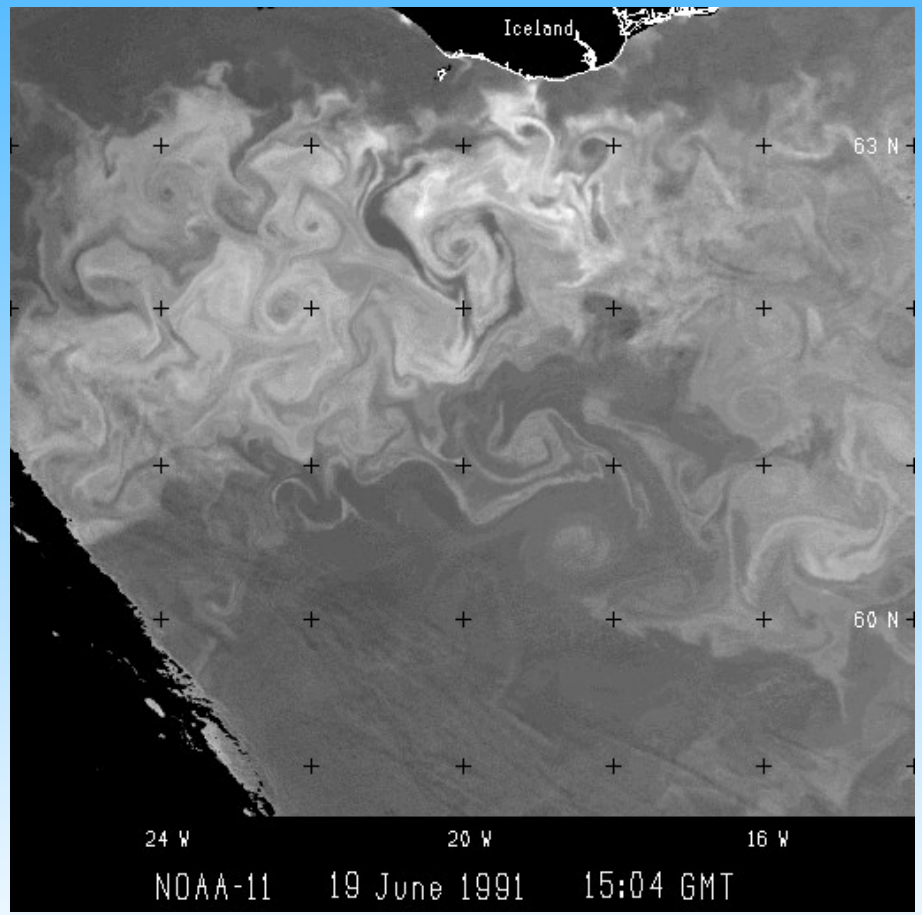

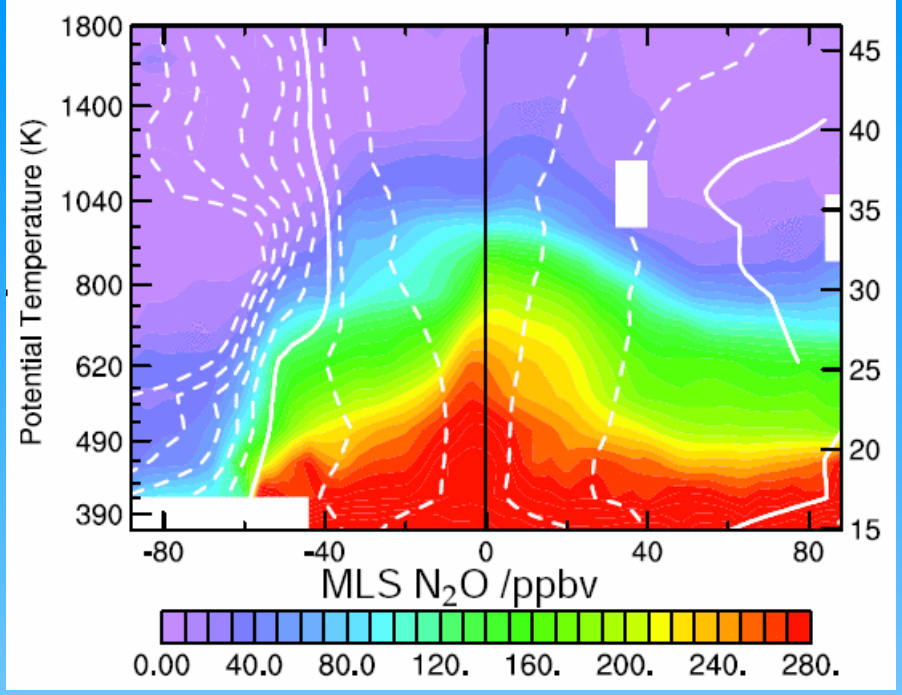

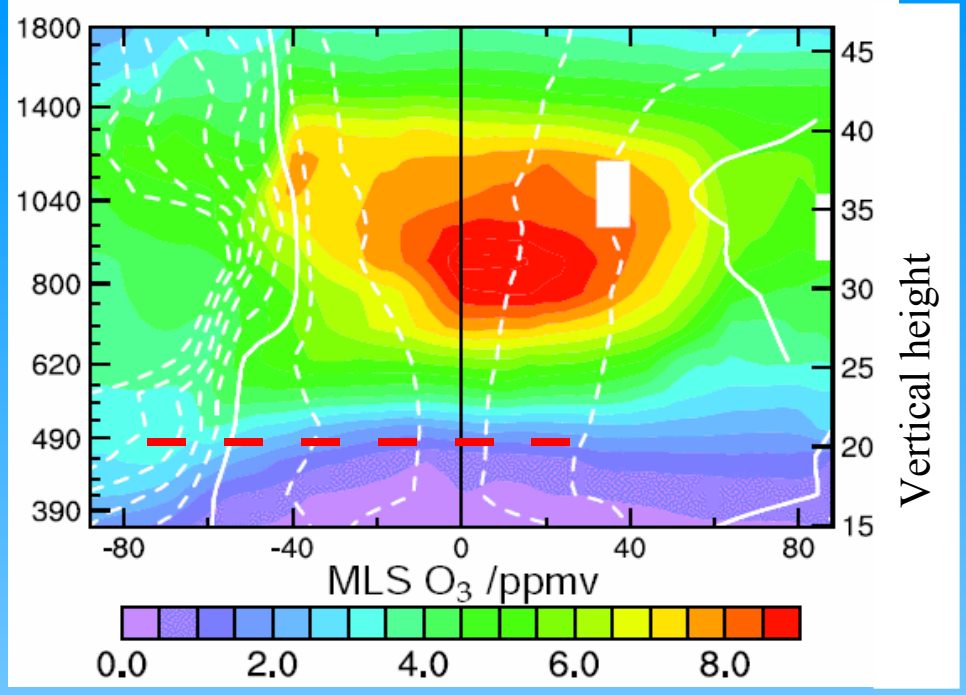

Gloria Manney, JPL, Caltech/NASA

Zonally averaged meridional sections of N_20 and O_3 from MLS-AURA.
3 August 2006

White contours: scaled PV

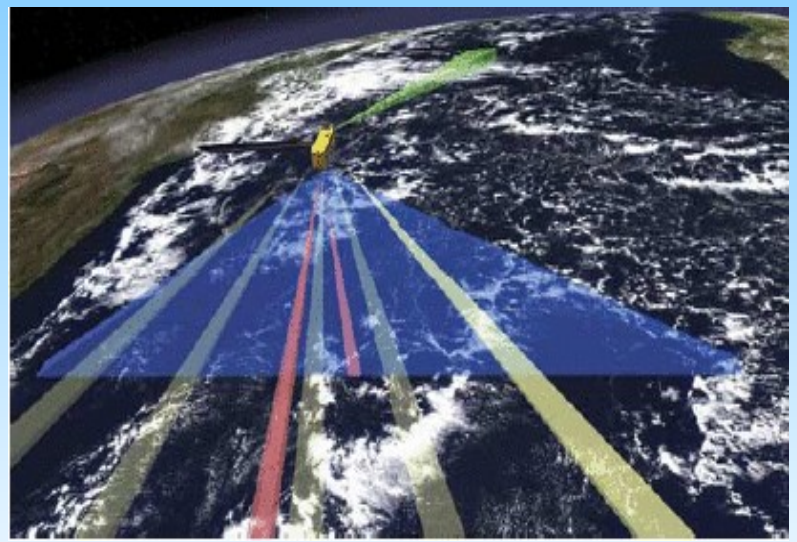

Artistic view of the MLS limb sounder in operation

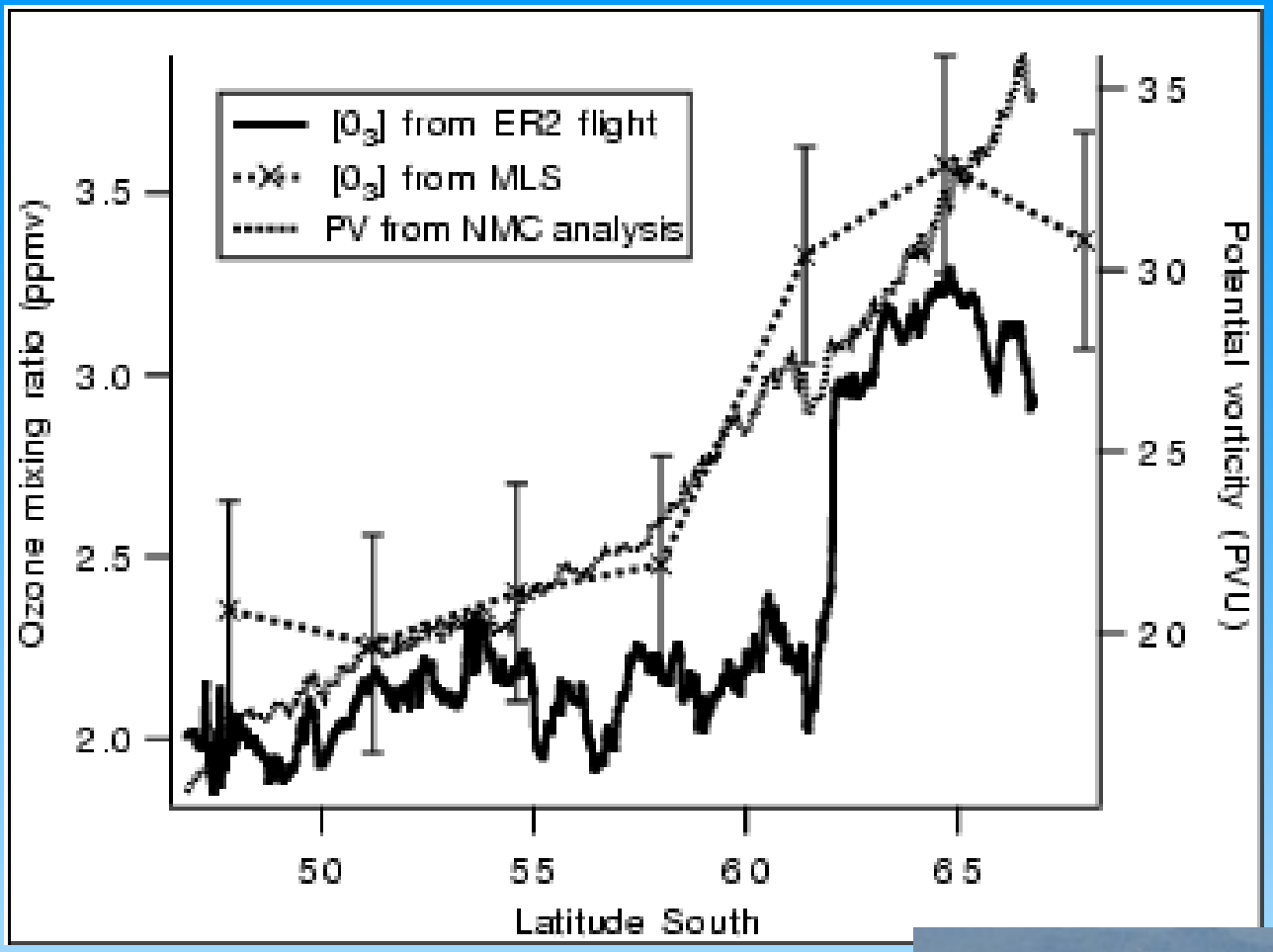

NASA ER-2 transect
across the edge of the
Antarctic polar vortex

sharp transition over a few km

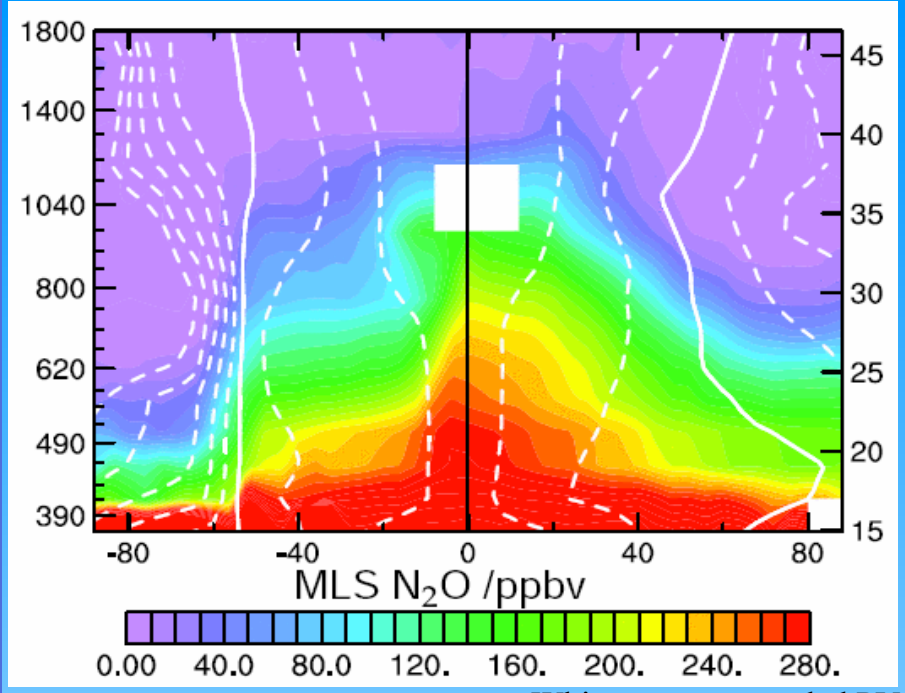

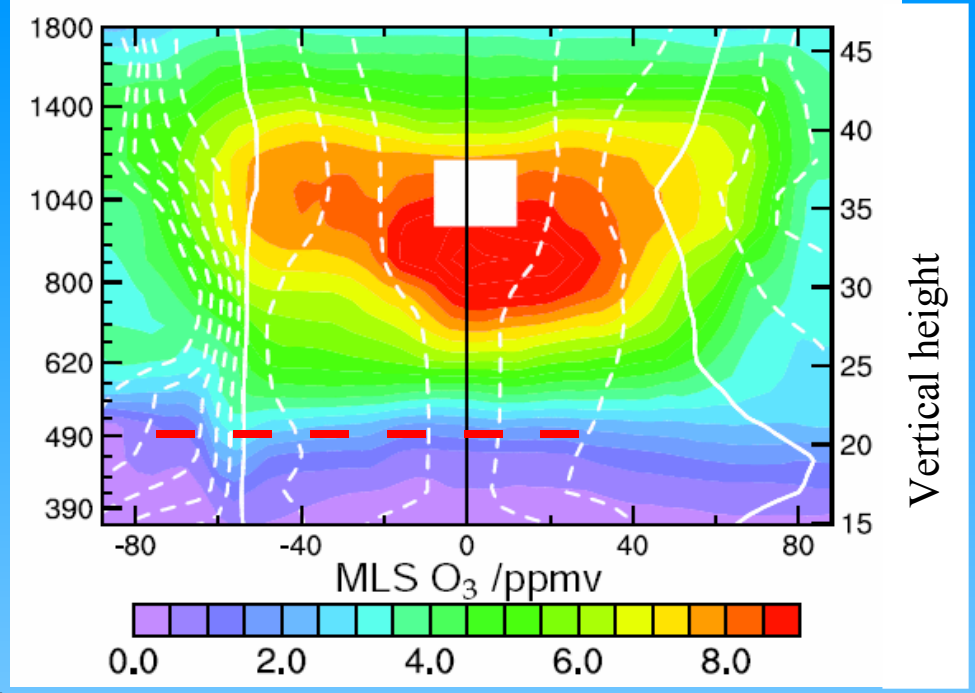

White contours: scaled PV
Black: temperature

MLS AURA
15 September 2006

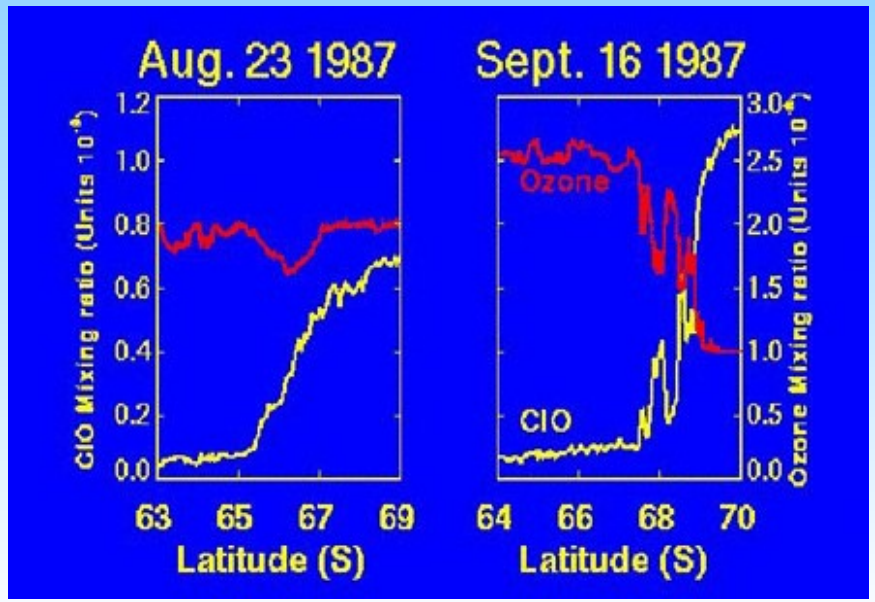

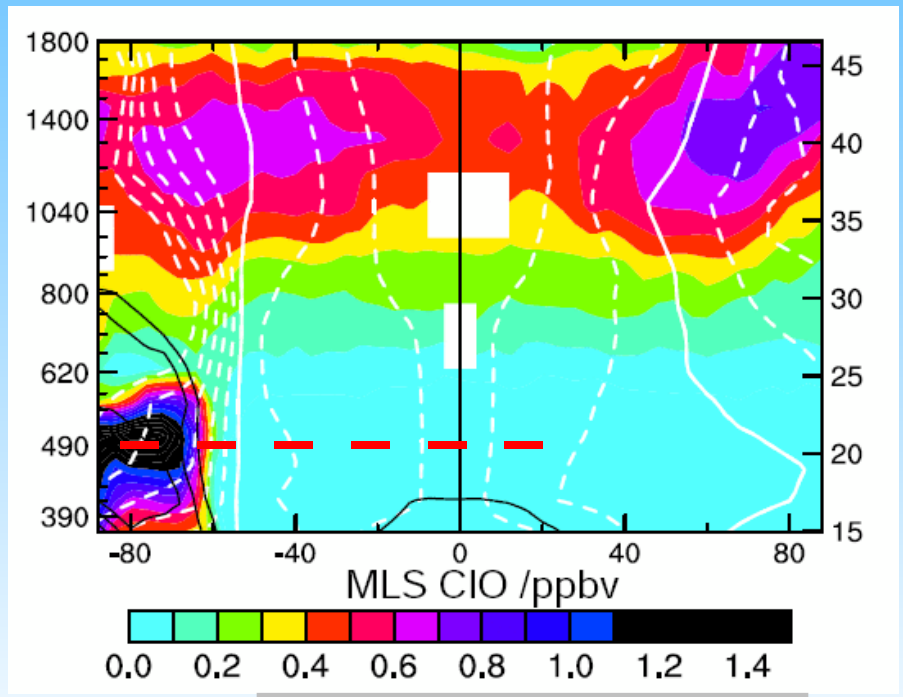

Gloria Manney, JPL, Caltech/NASA

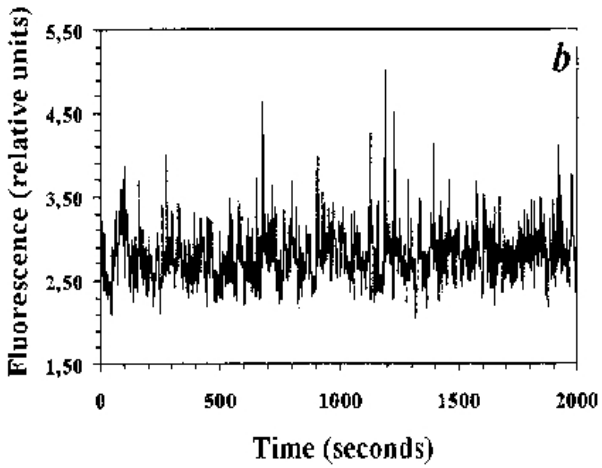

In vivo fluorescence at a fixed station in the English Channel.
Seuront et al., Nonlinear Proc. In Geophys. 3, 236 (1996).

In situ measurements exhibit a large amount of small-scale fluctuations, that are still poorly represented by models

N2O measured from aircraft in the stratosphere

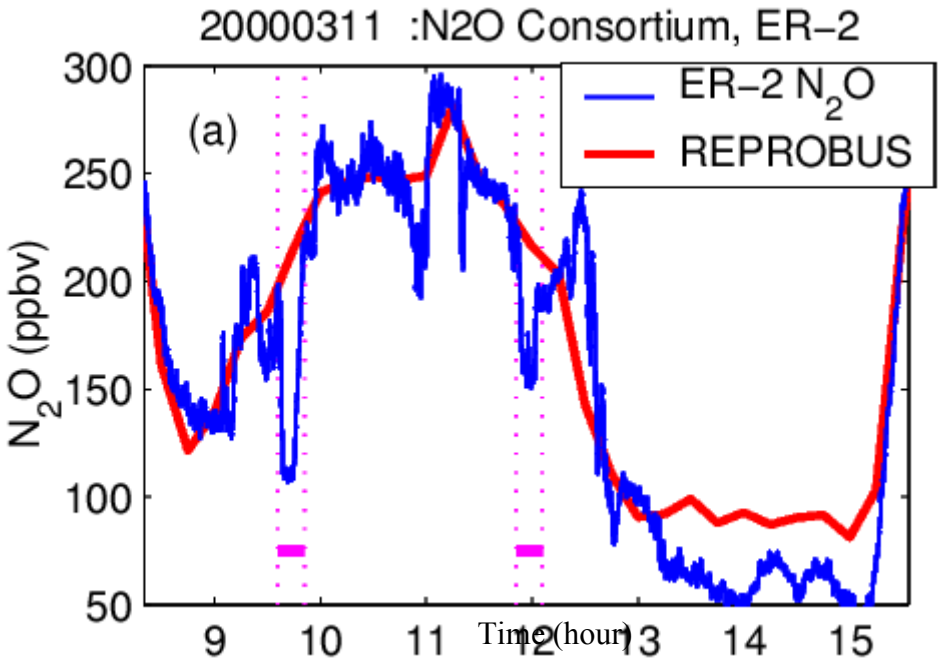

Hence, it is both interesting from the theoretical point of view and challenging from the practical point of view to understand the distribution of tracers in geophysical flows.

II.4

Ubiquity of quasi-horizontal layers in the troposphere

Reginald E. Newell*, Valerie Thouret*†, John Y. N. Cho*, Patrick Stoller*‡, Alain Marenco† & Herman G. Smit§

Nature, 25 March 1999

About 15% of the atmosphere is occupied by layers.

Mainly due to stratospheric intrusions

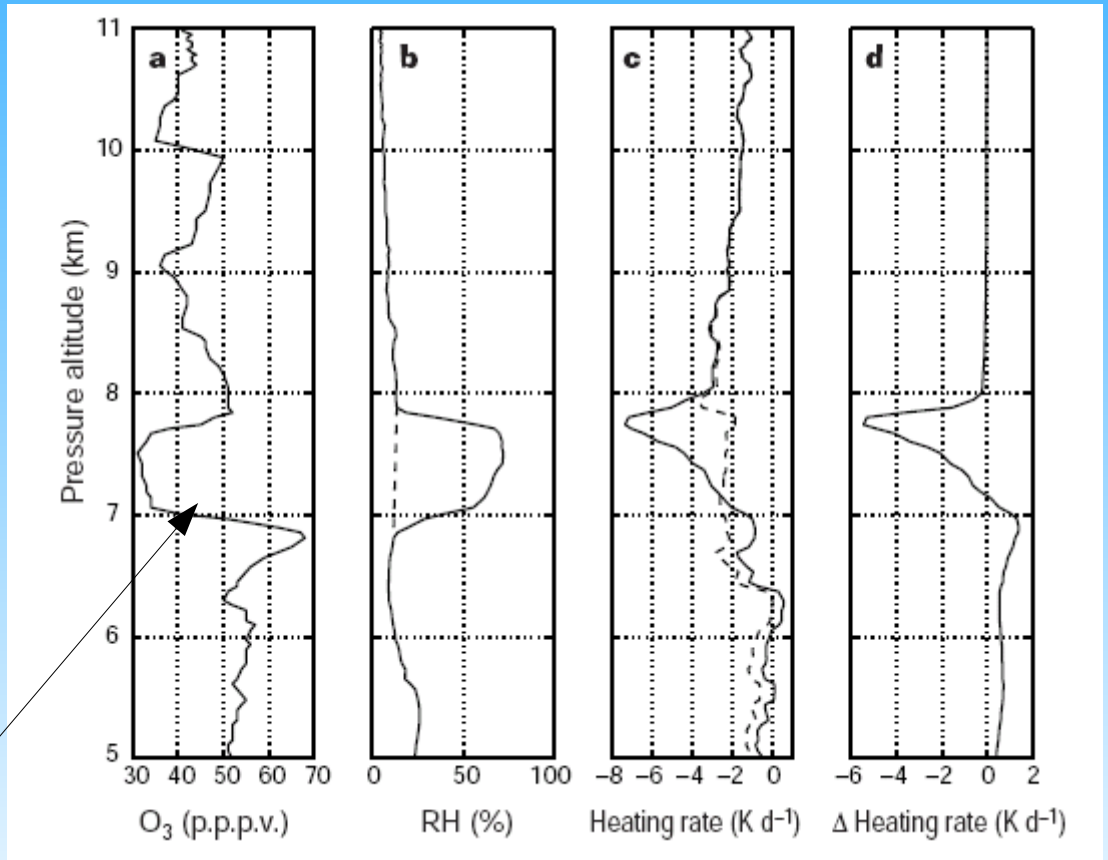

Ozone layer in the troposphere a few km under the tropopause

Example of layering in the free troposphere

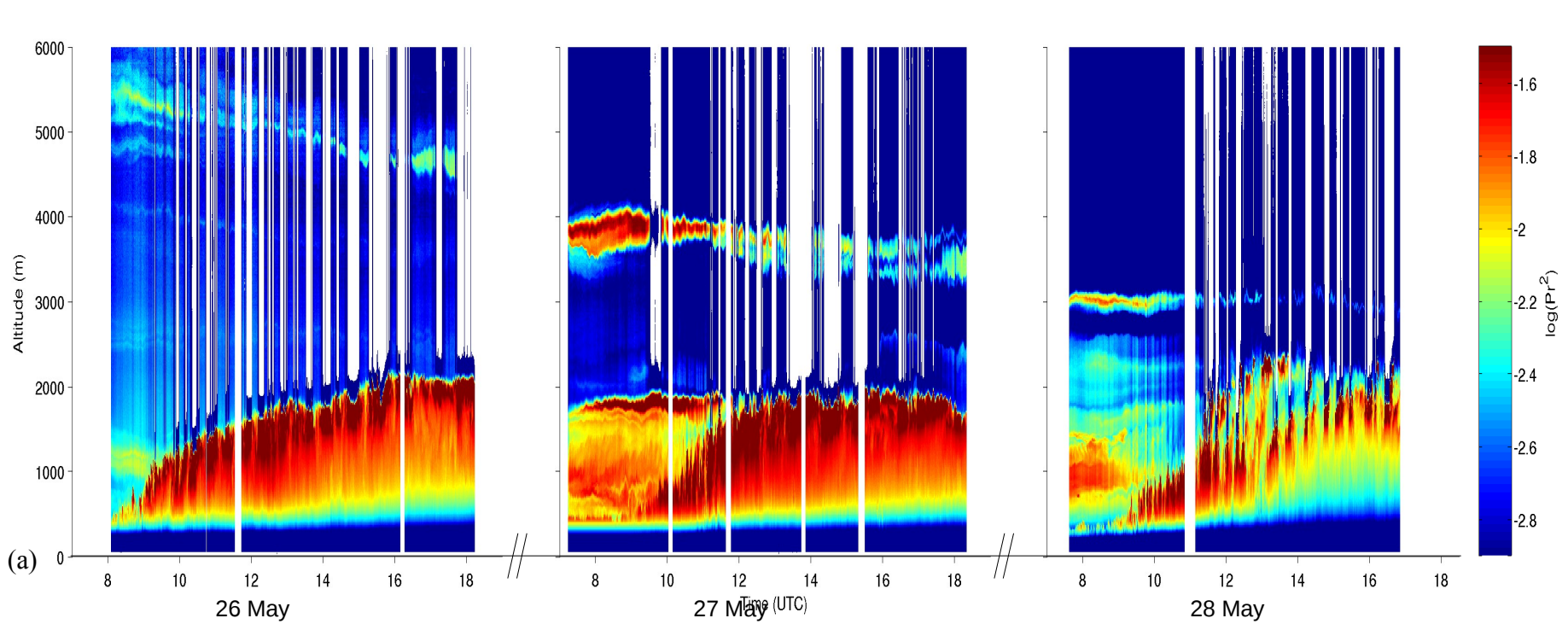

SIRTA aerosol lidar on 26-28 May 2003
Ecole Polytechnique / LMD

Transport et mélange

I Introduction et exemples

II Eléments de théorie

III Reconstructions des champs de traceurs

IV Barrières de transport

V Diagrammmes traceur-traceur et lignes de mélange

V Un exemple de méthode semi-lagrangienne

II. 1 Dispersion de particules - Marche au hasard

$\delta x = w_i \delta t$

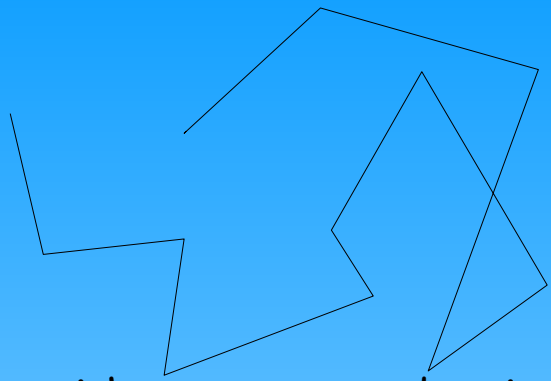

White noise, zero mean, variance σ

$$\langle w_i w_j \rangle = \sigma_w^2 \delta_{ij}$$

Displacement over N steps, or time $T = N \delta t$

$$X = \sum_{i=1}^{N} \delta x_i = \left(\sum_{i=1}^{N} w_i \right) \delta t$$

By central limit theorem, X is a Gaussian random process with zero mean and variance

$$\langle X^2 \rangle = N \sigma_w^2 \delta t^2 = (\sigma_w^2 \delta t) T$$

Hence, the p.d.f. $P_X(x,t)$ satisfies

$$\frac{\partial P}{\partial t} = \kappa \Delta P_X(x,t) \quad \text{with } P_X(x,0) = \delta(x),$$

which has solution $P_X(x,t) = \frac{1}{(2\kappa t)^{d/2}} \exp\left(\frac{-x^2}{4\kappa t} \right)$

provided $\kappa = \frac{1}{2} \sigma_w^2 \delta t$

If δt is not constant but jumps are of duration τ_i, the random process is over δx with variance σ_x. A necessary condition is than $\langle \tau \rangle$ is finite for which $\kappa = \frac{\sigma_x^2}{2\langle \tau \rangle}$

By adding advection by U we obtain the Fokker-Planck equation

$$\frac{\partial}{\partial t} P_X + U . \nabla P_X = \kappa \Delta P_X$$

which is also the advection-diffusion equation for the passsive tracer

Dispersion lagrangienne (Taylor)

We neglect here molecular diffusion and show that at large scales where dispersion exceeds the size of most energetic eddies, transport is again diffusive.

In Lagragian coordinates, motion of a parcel is

$$\boldsymbol{x}(\boldsymbol{a},t)=\boldsymbol{x}(\boldsymbol{a},0)+\int_0^t \boldsymbol{u}(\boldsymbol{x}(\boldsymbol{a},s),s)\,ds$$

where $x(\boldsymbol{a},t)$ is position at time t of parcel which was in $\boldsymbol{a}$ at time 0 (hence $\boldsymbol{x}(\boldsymbol{a},0)=\boldsymbol{a}$)

For each parcel with initial position $\boldsymbol{a}_i$, define

$$\boldsymbol{x}_i(t)=\boldsymbol{x}(a_i,t) \text{ and } \boldsymbol{v}_i(t)=\boldsymbol{u}(\boldsymbol{x}(\boldsymbol{a}_i,t),t)$$

Hence, $\frac{d}{dt}(\boldsymbol{x}_i-\boldsymbol{a}_i)^2=2(\boldsymbol{x}_i-\boldsymbol{a}_i)\boldsymbol{v}_i=2\int_0^t \boldsymbol{v}_i(t)\boldsymbol{v}_i(s)\,ds$,

and after averaging over ensemble

$$\frac{d}{dt}\langle(\boldsymbol{x}_i-\boldsymbol{a}_i)^2\rangle=2\int_0^t S(t-s)\,ds=2\int_0^t S(s)\,ds$$

where $S(t-s)=\langle \boldsymbol{v}_i(t)v_i(s)\rangle$ is the Lagrangian velocity correlation, assuming homogeneity and stationnarity.

This can be solved as

$$\langle(\boldsymbol{x}_i-\boldsymbol{a}_i)^2\rangle=2\int_0^t (t-s)\,S(s)\,ds$$

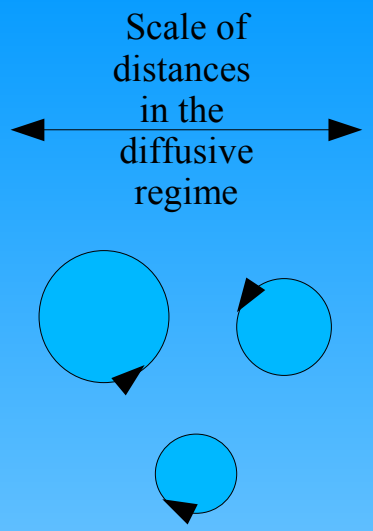

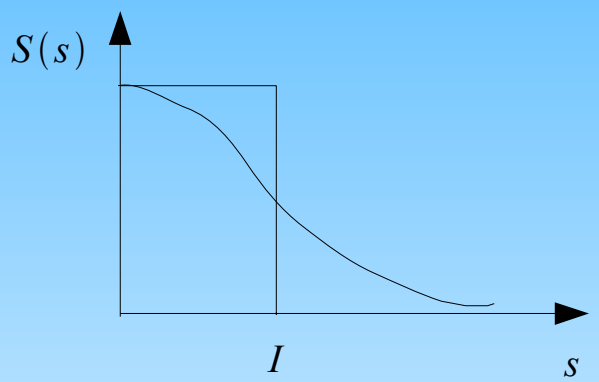

Integral scale I

$$\int_0^\infty S(s)\,ds=\langle v^2\rangle I$$

Diffusive regime: If $S(s)$ decays fast enough, and for $t \gg I$

$$\langle (\boldsymbol{x}_i - \boldsymbol{a}_i)^2 \rangle \sim 2\,Dt \text{ with } D = \int_0^\infty S(s)\,ds$$

If the integral $\int_0^\infty S(s)\,ds$ diverges, the diffusive regime does not exist.

For instance if $S(s) \sim s^{-\eta}$ with $0 < \eta < 1$, the regime is super-diffusive

$$\langle \boldsymbol{x}^2 \rangle \sim t^{2-\eta}$$

If now $\int_0^\infty S(s)\,ds = 0$, but if $\int_0^t (t-s)\,S(s)\,ds$ diverges with t, we have a sub-diffusive regime. For instance if $S(s) \sim s^{-\eta}$ with $1 < \eta < 2$ for large enough times, we have again $\langle \boldsymbol{x}^2 \rangle \sim t^{2-\eta}$ but with an exponent less than 1

Application:
Profil d'un panache à distance de la source

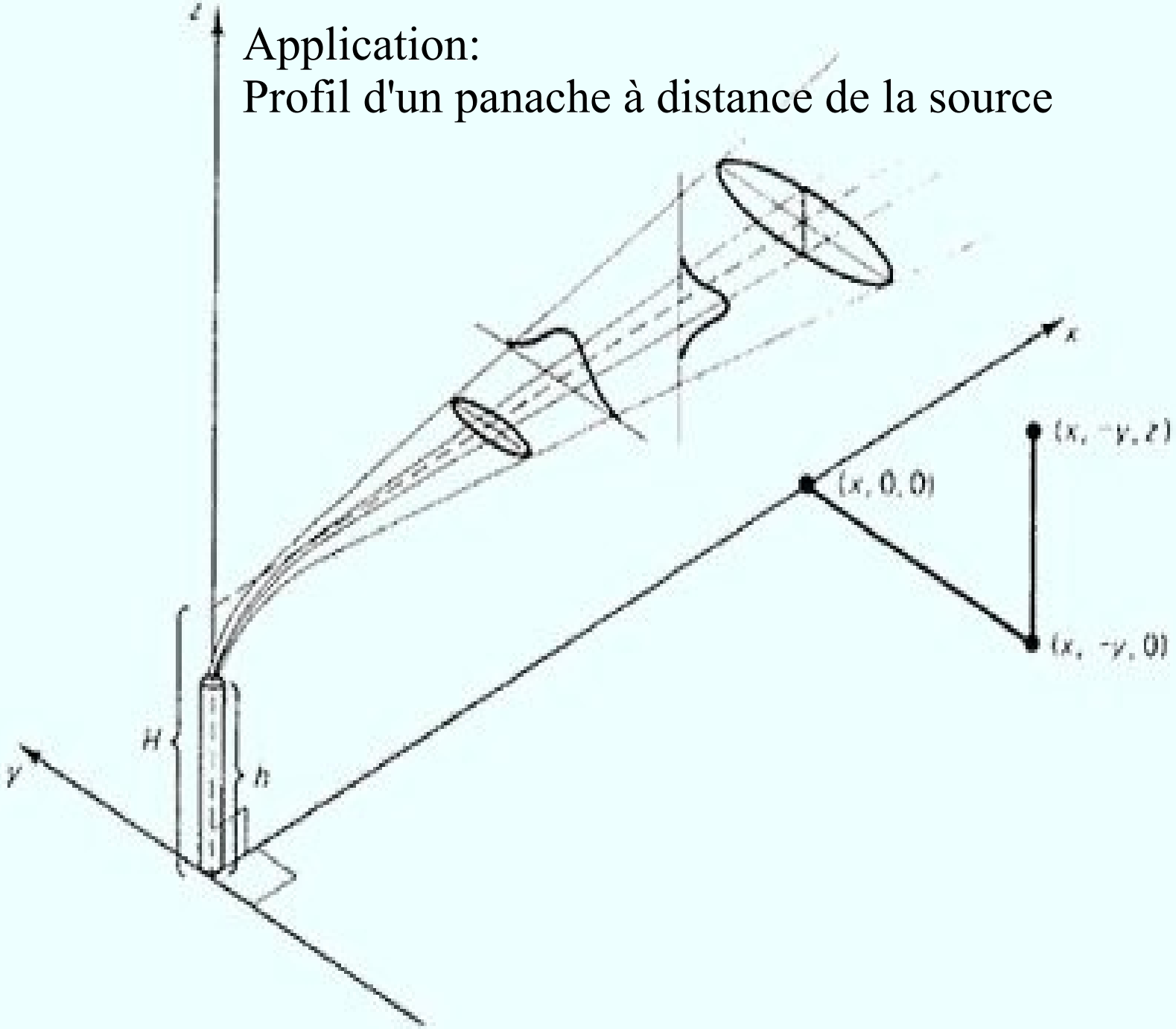

Figure 2: Plume Dispersion by Gaussian Distribution and Coordinate System.

Croissance de la taille latérale σ_y du panache en fonction du temps

et diffusion turbulente $K = \frac{1}{2}\frac{d\,\sigma_y^2}{d\,t}$

pour différents régimes de la turbulence.

Dans la couche de surface où $u = \frac{u^*}{\kappa}\log\frac{z}{z_0}$

$$\sigma_y = C_1 u^* t \qquad\qquad K \sim u^* \sigma_y$$

Dans la zone inertielle de Kolmogorov gouvernée par le taux de dissipation d'énergie turbulente ϵ

$$\sigma_y = C_2 \epsilon^{1/2} t^{3/2} \qquad\qquad K \sim \epsilon^{1/3} \sigma_y^{4/3}$$

A l'échelle supérieure aux toubillons énergétiques

$$\sigma_y = \sqrt{2\,D\,t} \qquad\qquad K = D$$

Dispersion dans l'océan

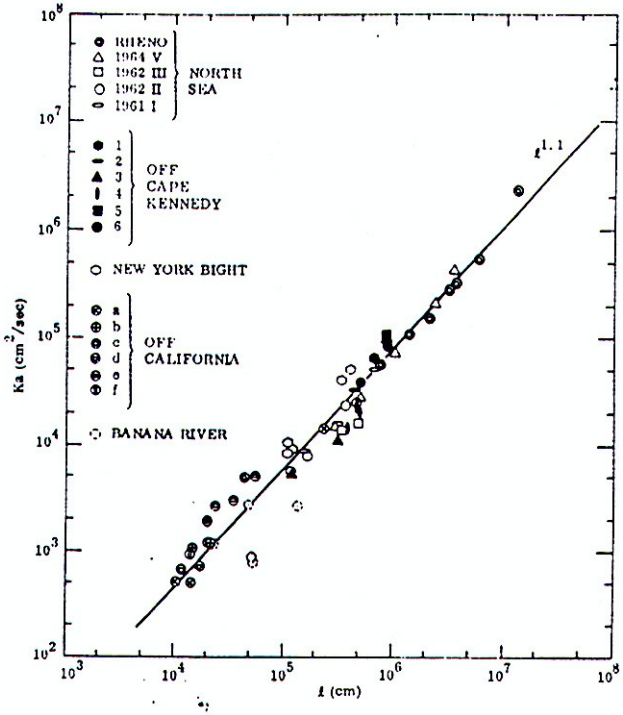

Fig. 4.9. A diffusion diagram for apparent diffusivity vs. scale of diffusion (from Okubo, 1971).

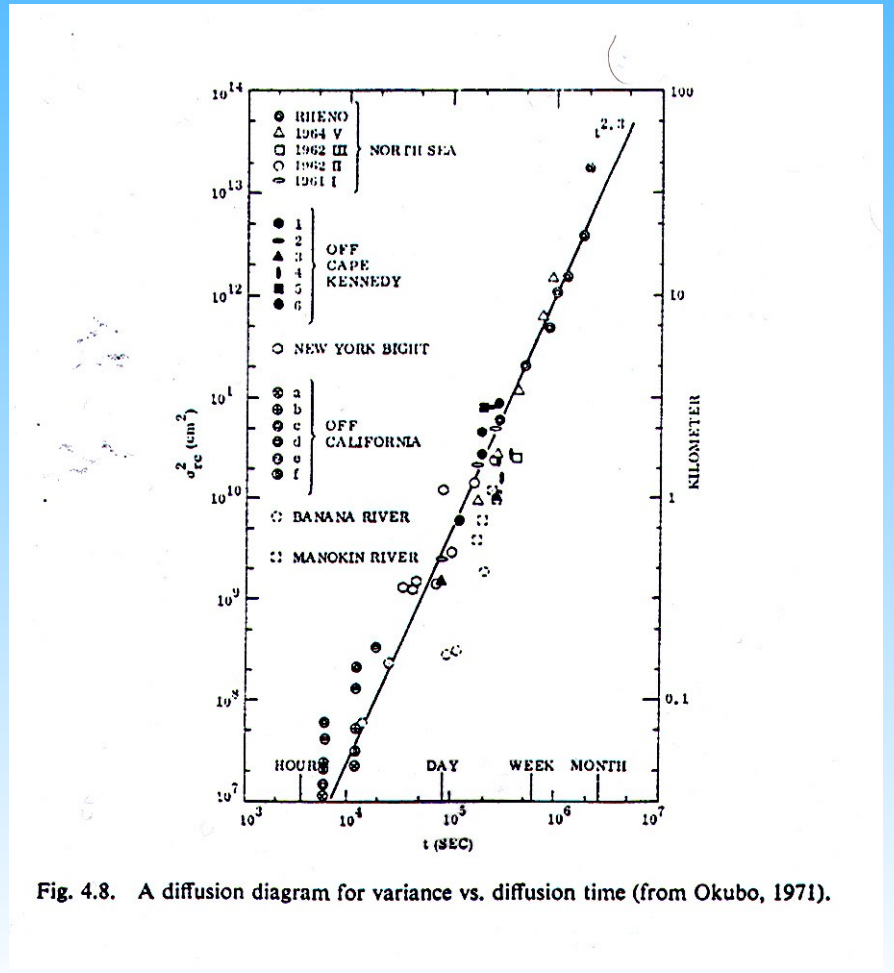

Fig. 4.8. A diffusion diagram for variance vs. diffusion time (from Okubo, 1971).

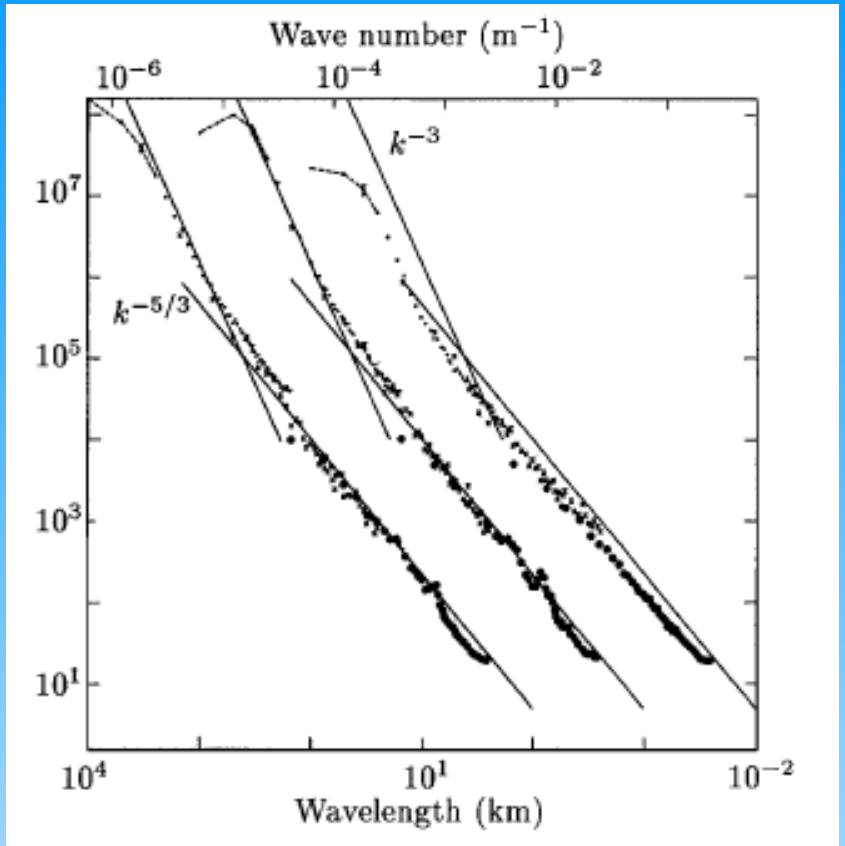

FIG. 1. From left to right: variance power spectra of zonal wind, meridional wind ($m^3\ s^{-2}$), and potential temperature (K^2 m) near the tropopause from Global Atmospheric Sampling Program aircraft data. The spectra for meridional wind and temperature are shifted one and two decades to the right, respectively. Reproduced from [7].

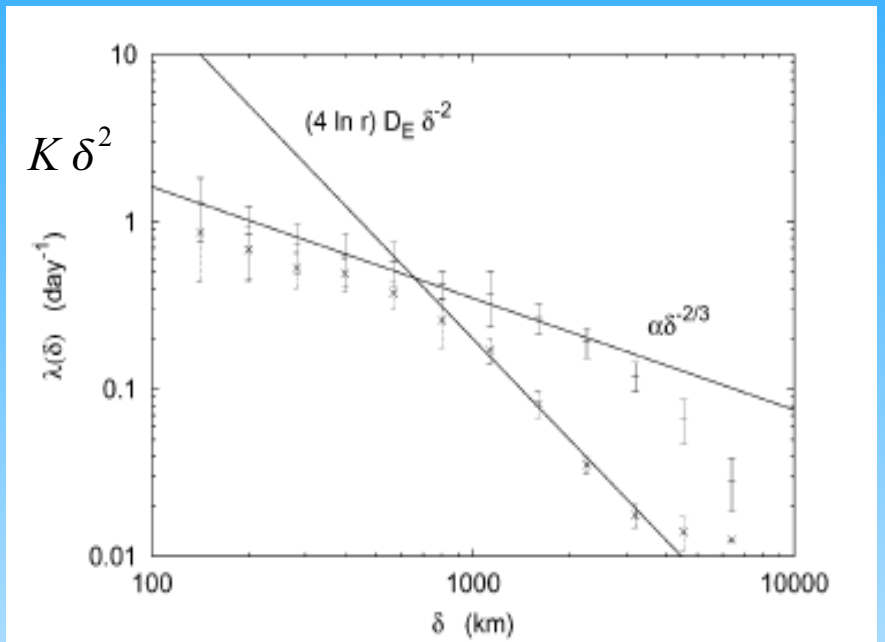

FIG. 5. FSLE of the balloon pairs, (–) describing total and (×) meridional dispersion, with initial 100-km threshold. The meridional FSLE is λ_{mer} defined in Eq. (2.7). The meridional eddy diffusion coefficient is $D_E \simeq 1.5 \times 10^6\ m^2\ s^{-1}$.

Nastrom & Gage, J. Atmos. Sci., 1985

II.2 Mélange chaotique versus turbulent

- Mélange turbulent dans les écoulements inertiels en 3D avec un grand nombre de degrés de liberté excités
- Lois d'échelle de Kolmogorov
  - incrément de vitesse $\delta U(r) \sim r^{1/3}$
  - Le gradient de vitesse est singulier dans la limite inviscide

- Brassage chaotique dans les écoulements en couche (quasi-2D) dominés pas l'advection de grande échelle
- Ecoulement de Batchelor
  - Incrément de vitesse $\delta U(r) \sim r$
  - Le gradient de vitesse est toujours borné

A GRANDE ECHELLE

Dispersion
par un
écoulement
atmosphérique

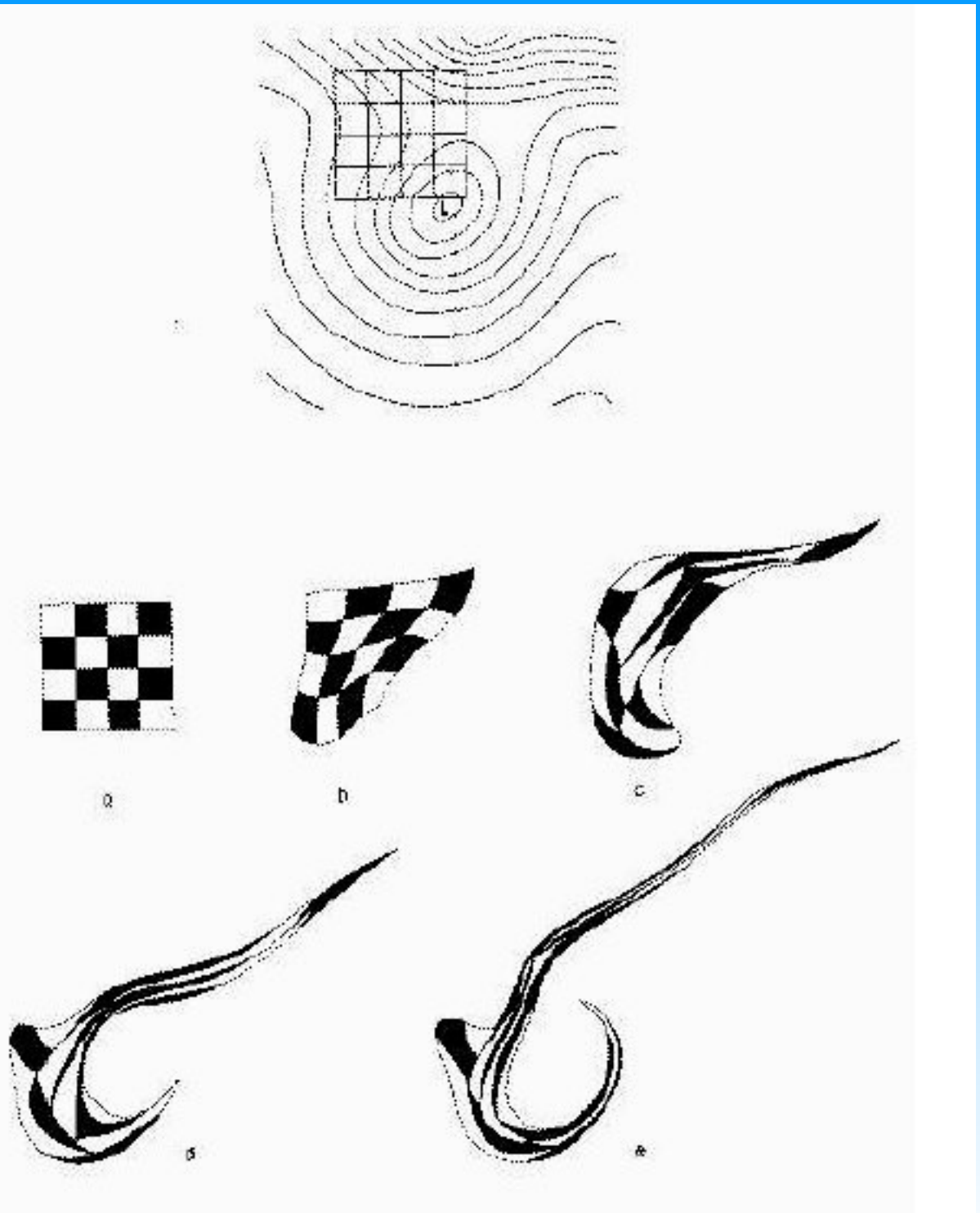

Déformation
par un écoulement
2D turbulent

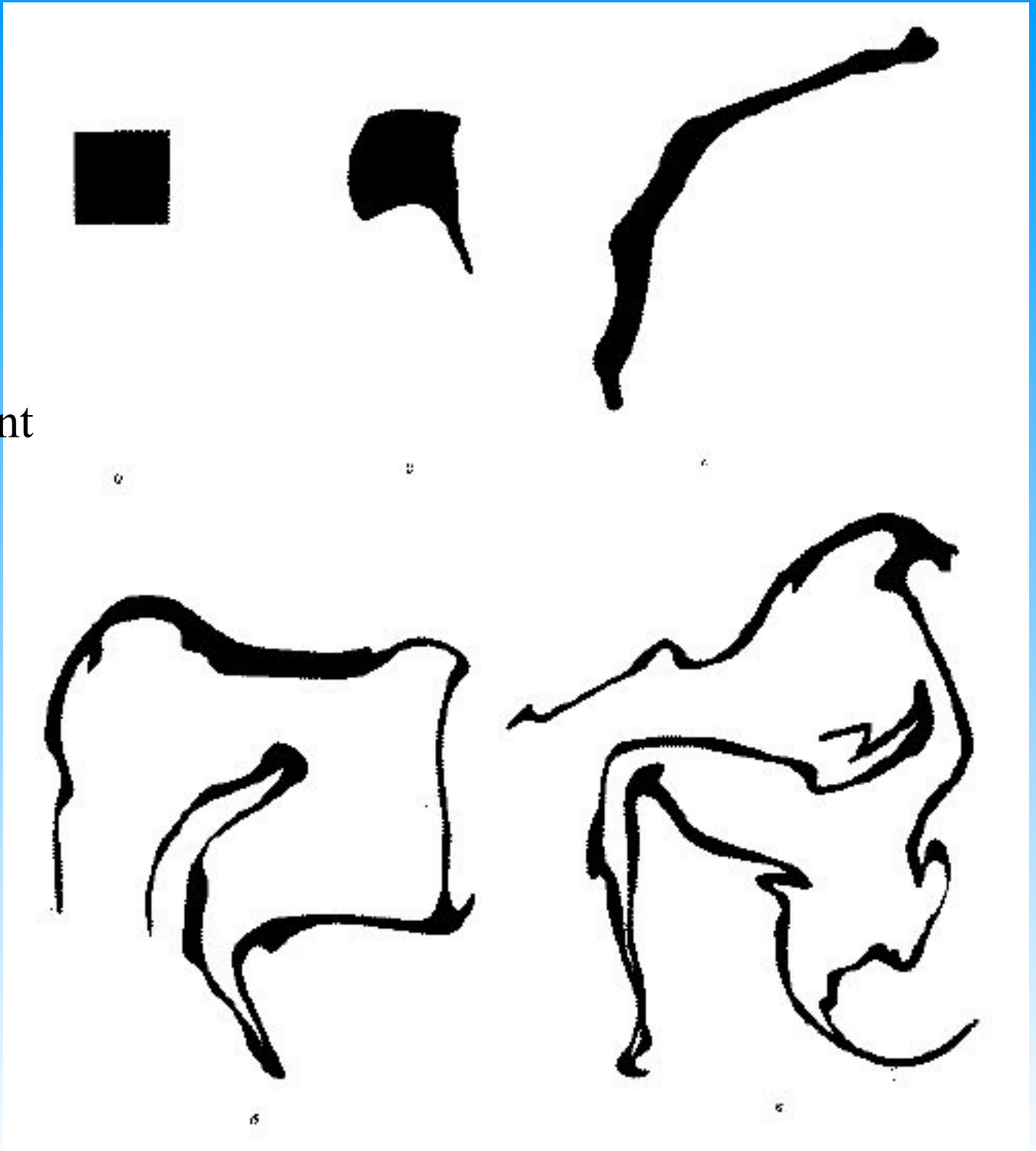

Efficient stirring is performed by a periodic flow

Trajectories may be chaotic in 2D for a periodic flow, in 3D for a stationary flow.

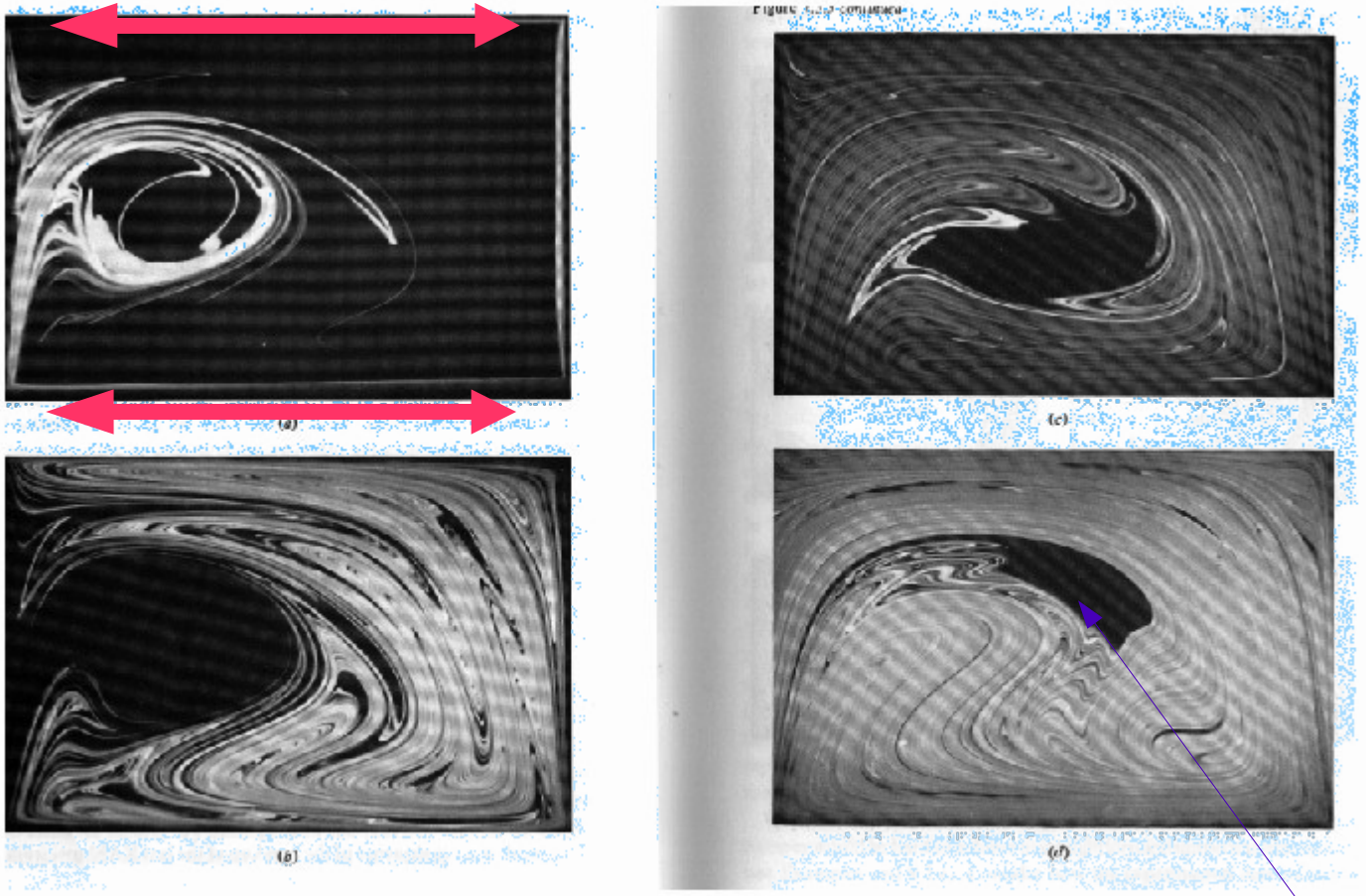

J.M. Ottino, The kinematics of mixing: stretching, chaos, and transport (Cambridge, 1989)

unmixed island

Lyapunov exponent

Evolution equations for a line element and the passive scalar gradient in the absence of diffusion and source are very similar since $\nabla\theta\cdot\mathbf{x}=\delta\theta$ is preserved

$$\frac{D}{Dt}\delta x_i=\frac{\partial u_i}{\partial x_j}\delta x_j \qquad \frac{D}{Dt}\frac{\partial\theta}{\partial x_i}=\frac{-\partial u_j}{\partial x_i}\frac{\partial\theta}{\partial x_j}$$

$\left(\frac{D}{Dt}\right.$ time derivation along a given trajectory $\left.\mathbf{x}(t)\right)$

Over a time interval $[t_0, t_0+\tau]$:

$$\delta\mathbf{x}(t_0+\tau)=\mathbf{M}(t_0, t_0+\tau)\,\delta\mathbf{x}(t_0) \qquad \nabla\theta(t_0+\tau)=-\mathbf{M}^T(t_0, t_0+\tau)\nabla\theta(t_0)$$

Finite-time Lyapunov exponent

$$\lambda(\tau,\mathbf{x}(t_0))=\frac{1}{\tau}\ln\frac{|\mathbf{M}\delta\mathbf{x}|}{|\delta\mathbf{x}|}=\frac{1}{\tau}\ln\frac{|\mathbf{M}^T\nabla\theta|}{|\nabla\theta|}$$

At large τ, if the flow is ergodic, $\lambda(\tau,\mathbf{x}(t_0))$ tends to a unique $\bar{\lambda}$.
At intermediate τ, λ exhibits large spatial and temporal variations.

Evolution of a tracer blob under the combined action of stretching and diffusion

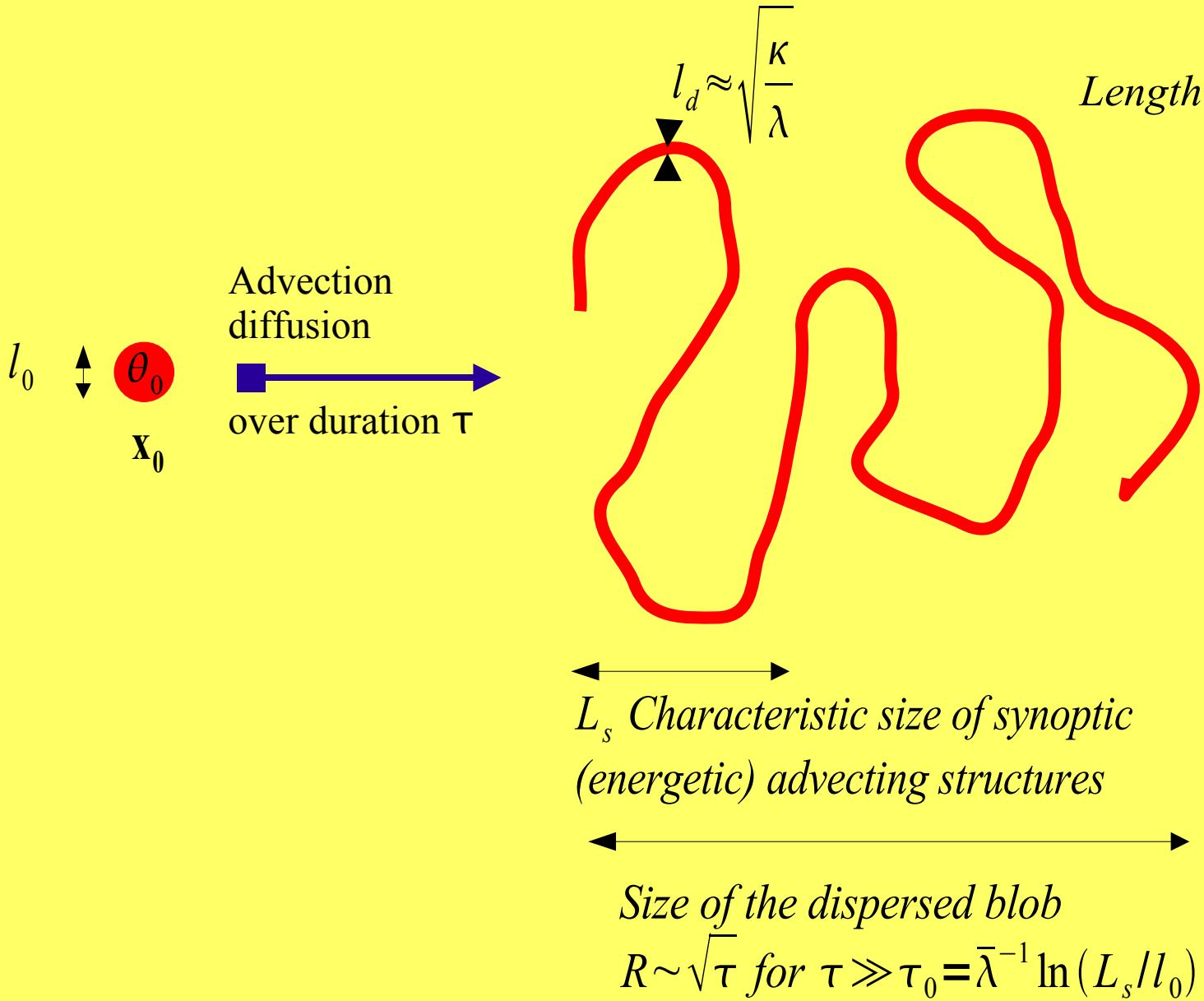

Transport et mélange

I Introduction et exemples

II Eléments de théorie

III Reconstructions des champs de traceurs

IV Barrières de transport

V Diagrammmes traceur-traceur et lignes de mélange

V Un exemple de méthode semi-lagrangienne

Appenzeller, Davies & Norton, 1996, JGR, D101(1), 1435-1456

Meteosat water-vapor

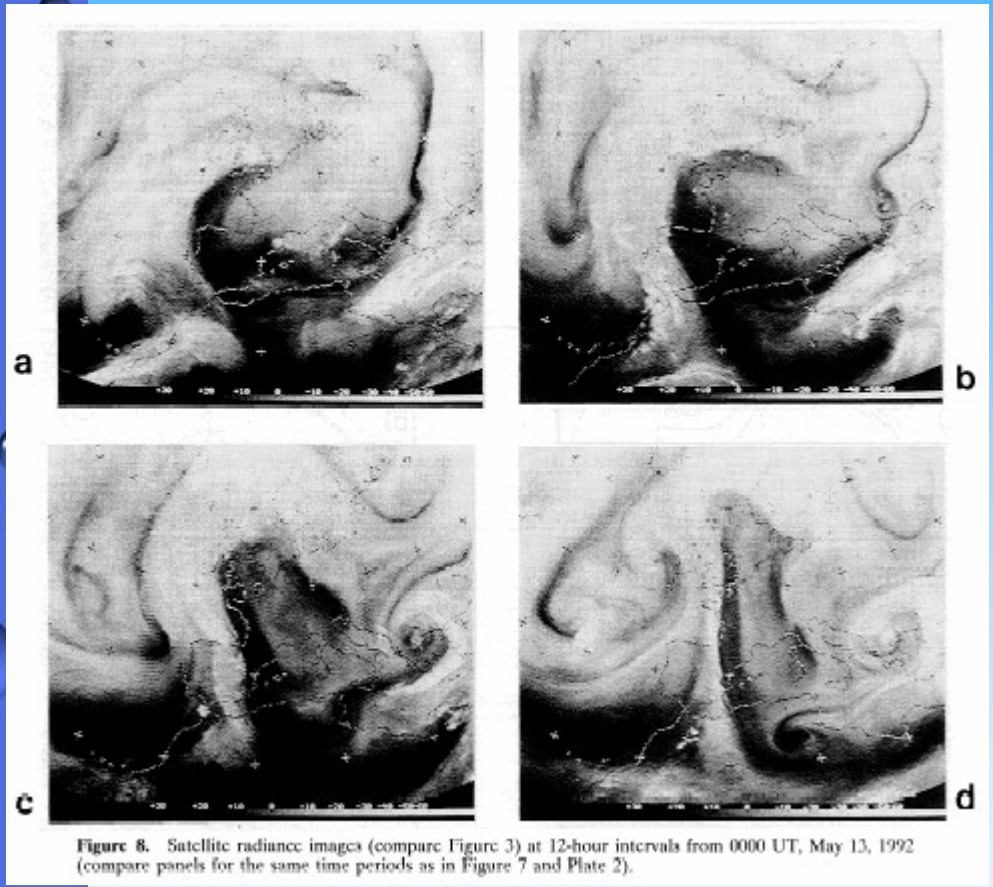

Figure 8. Satellite radiance images (compare Figure 3) at 12-hour intervals from 0000 UT, May 13, 1992 (compare panels for the same time periods as in Figure 7 and Plate 2).

PV reconstruction by isentropic contour advection at 320 K

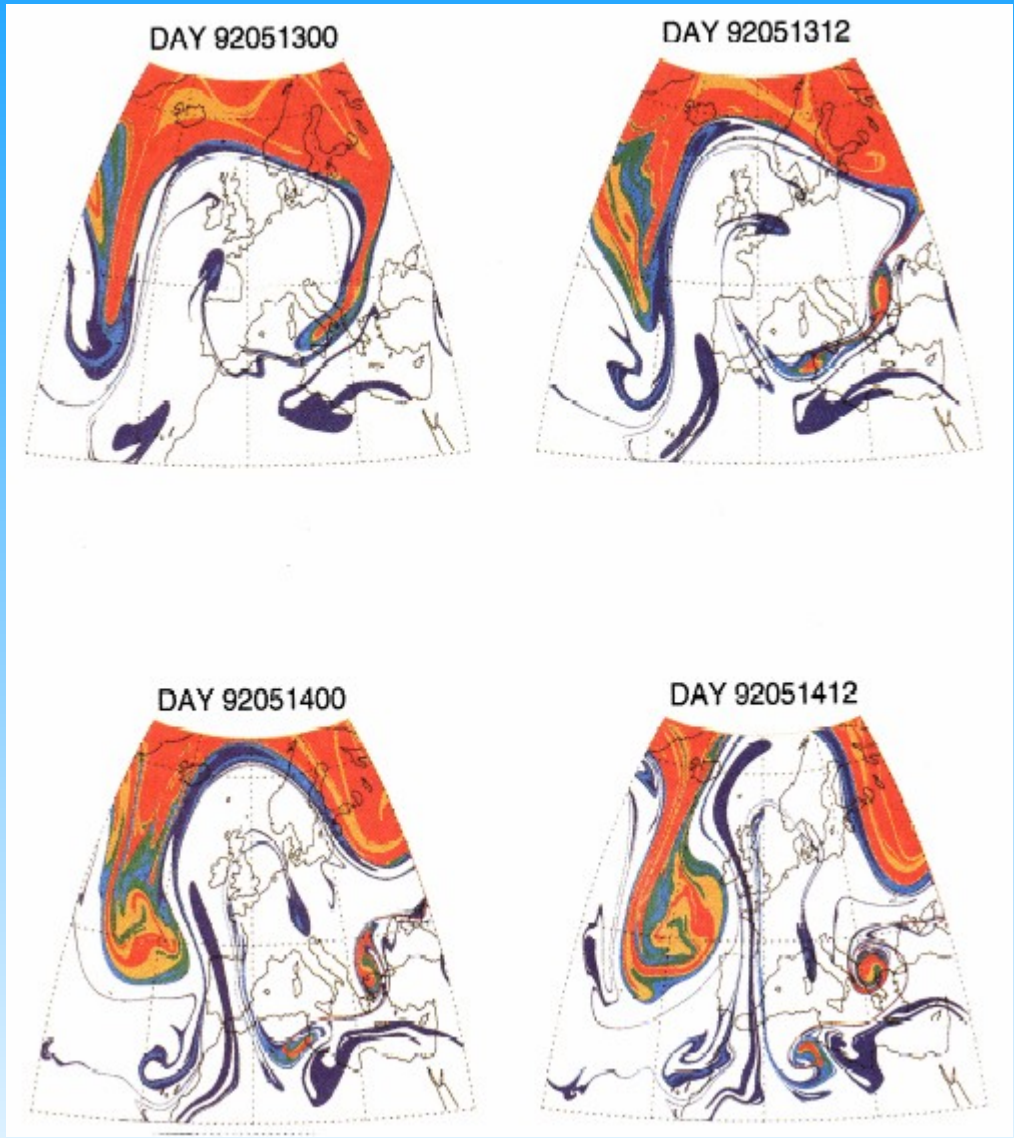

II.3 Reconstructions des champs de traceurs

Reconstruction of a tracer field is obtained by reverse time integration of particle trajectories initialised from their final position from t_0 to $t_0 - \tau$, using analysed winds (e.g. ECMWF winds).

- assignment of the chemical tracer value or PV at $t_0 - \tau$ location from low resolution CTM (chemical transport model) or analysed fields

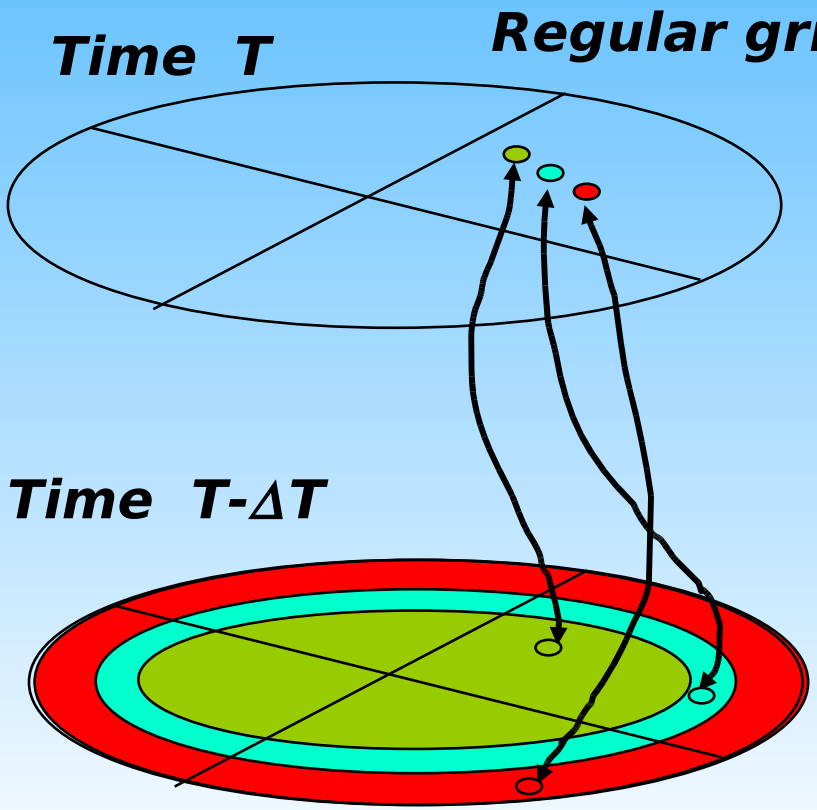

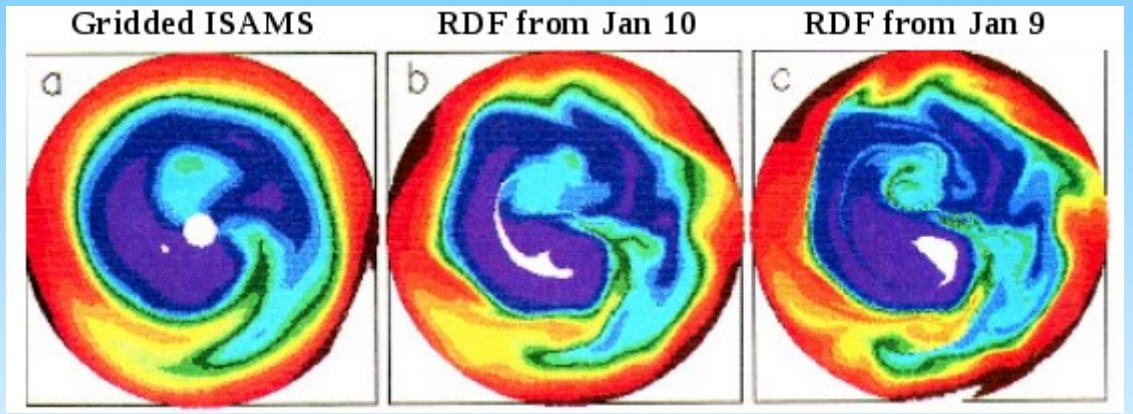

Vortex polaire et confinement

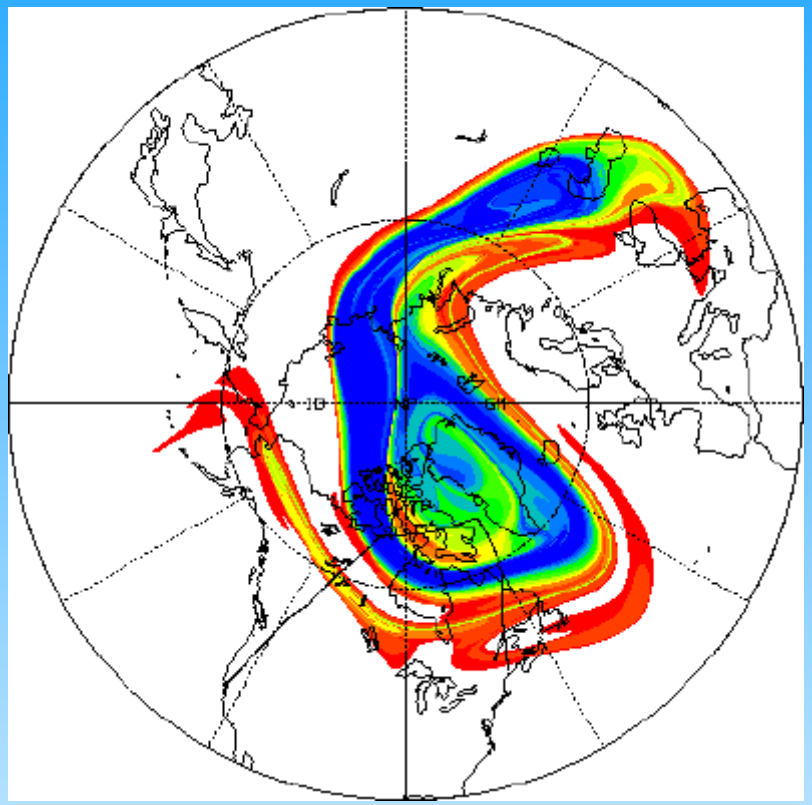

vortex polaire arctique
1992 (reconstruction
de la distribution d'un traceur)

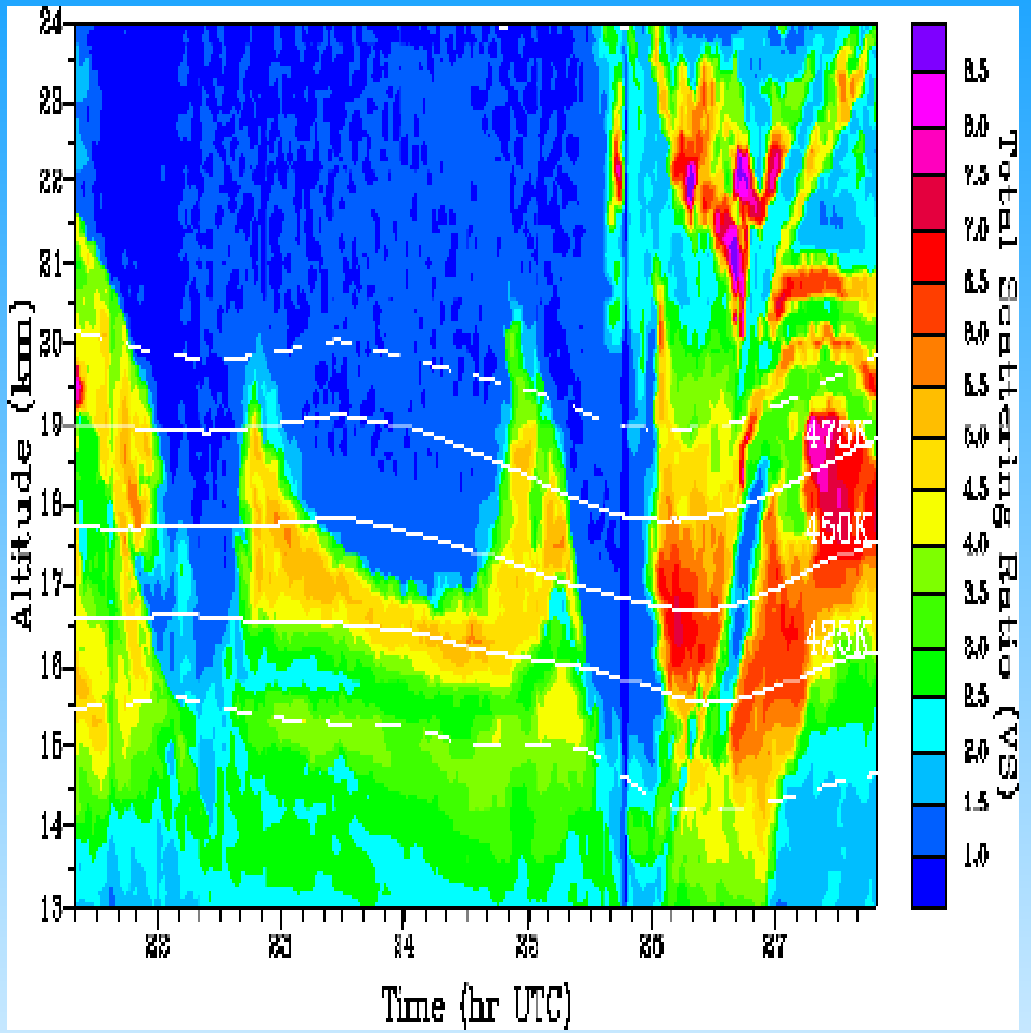

lidar aérosol embarqué
poussières issues du Pinatubo hors
du vortex polaire

Waugh et al, 1994, JGR D99(1), 1071-1088.

Mariotti et al., 1997, JGR D102, 6131-6142

Layerwise motion and the generation of filaments in the lower stratosphere -> laminae in the ozone vertical profile

PV reconstruction by isentropic advection

ozone profile from Lerwick

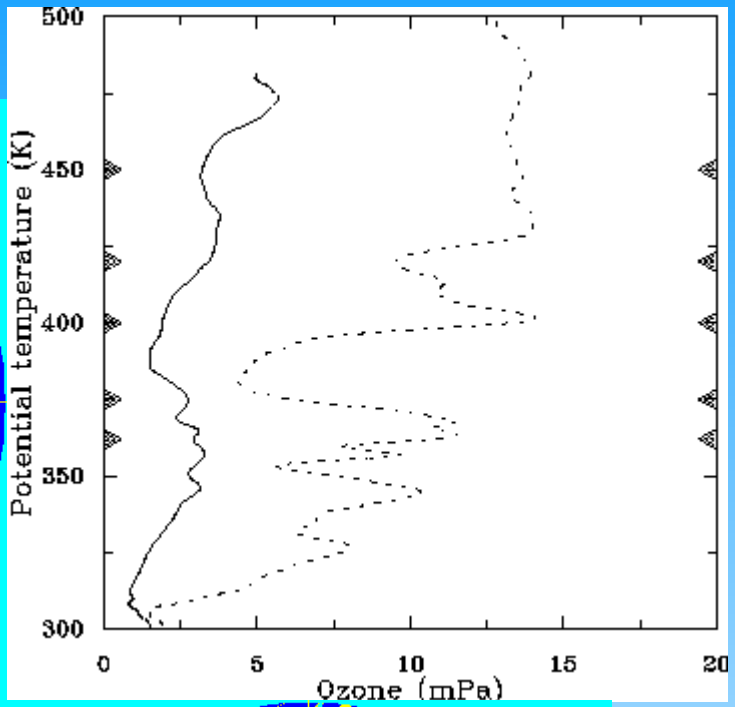

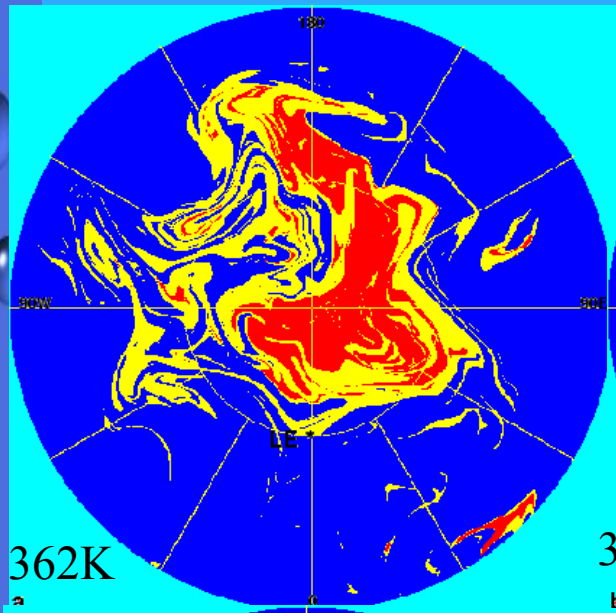

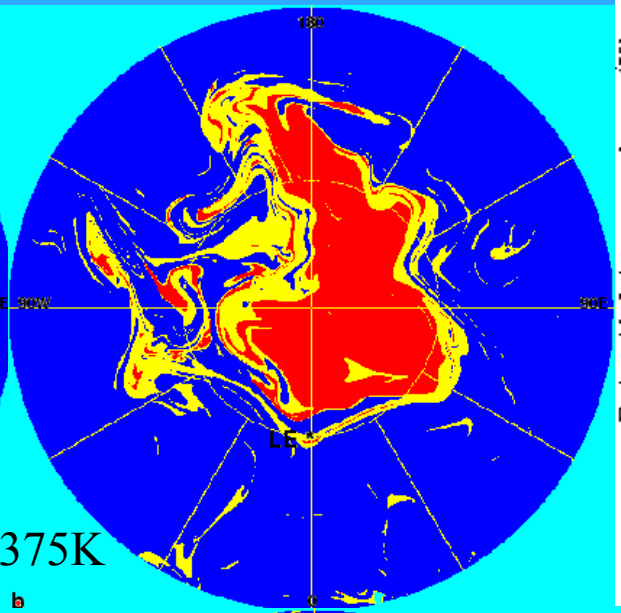

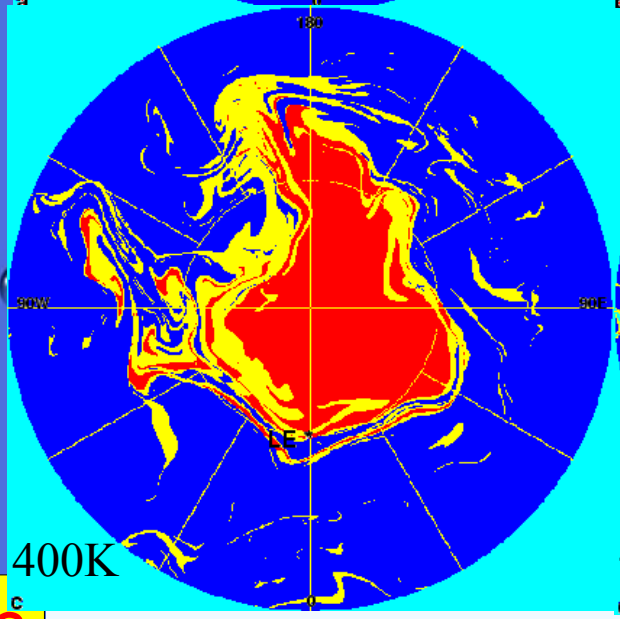

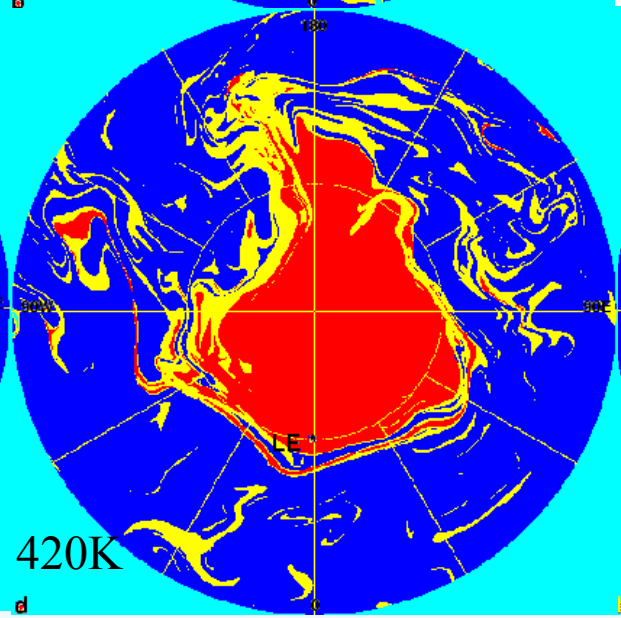

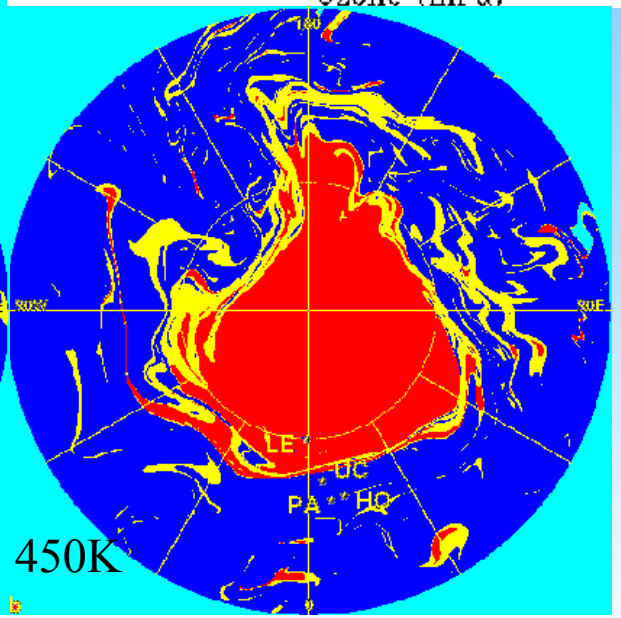

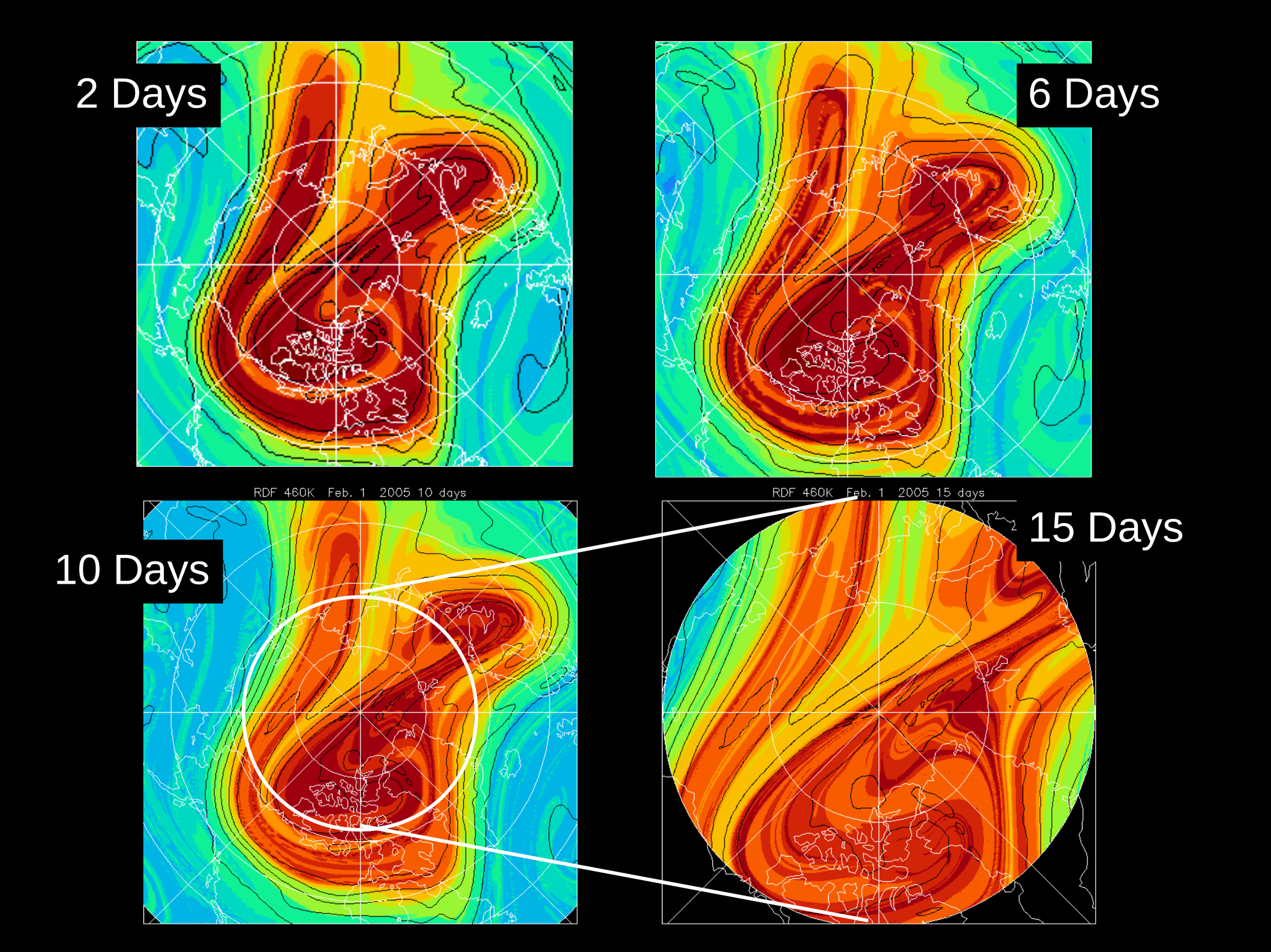
2 Days
6 Days
RDF 460K Feb. 1 2005 10 days
10 Days
RDF 460K Feb. 1 2005 15 days
15 Days

Observations

Reconstructions

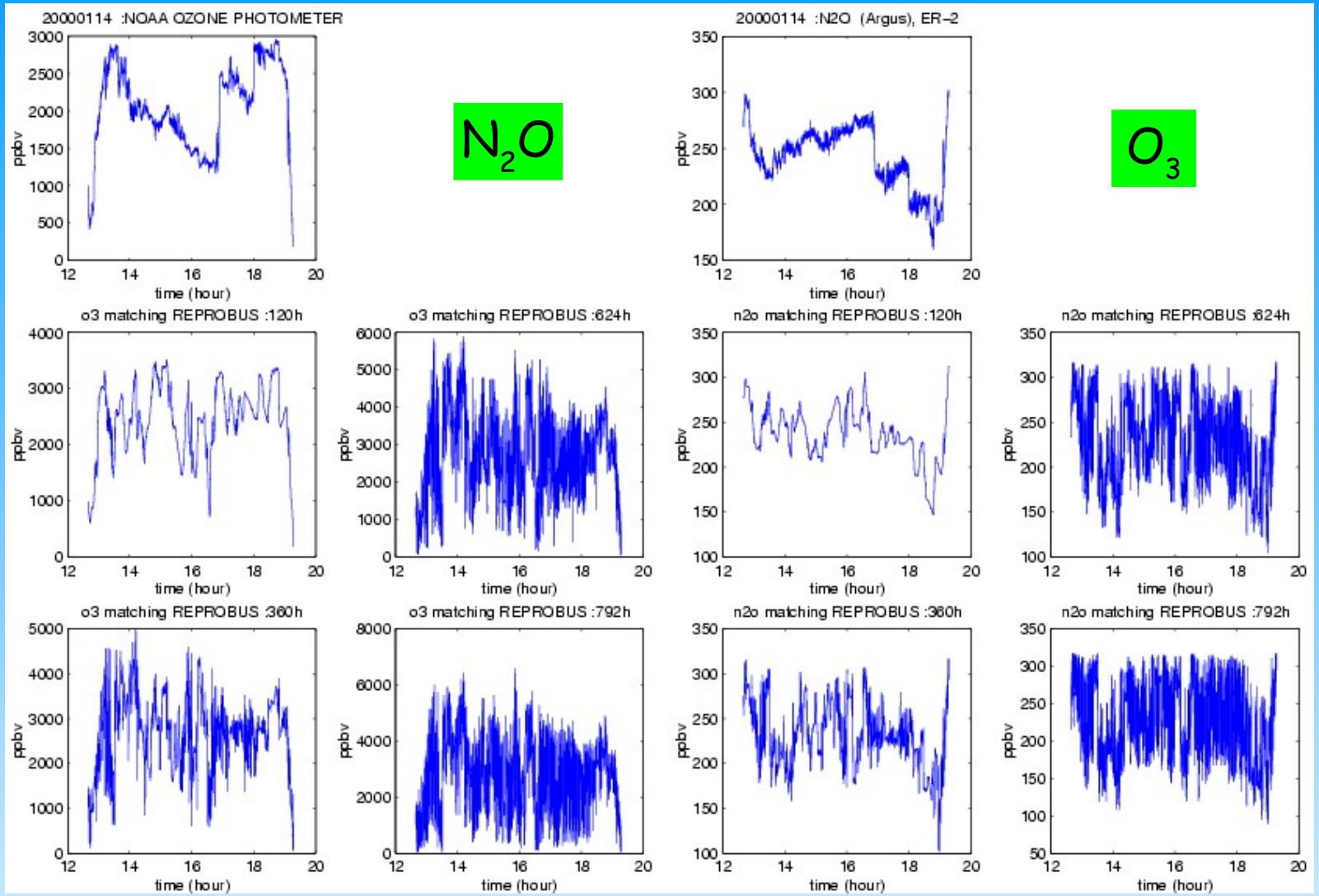

For comparison: deterministic reconstructions for τ = 5, 15, 26 and 33 days

Diffusion and random vertical motion

Let vertical motion be $\delta z = w\,\delta t + \eta\,\delta t$
where η *is a white noise and* δt
is the time step.
Over a large number of time steps,
this is equivalent to a diffusive
process with $D = \frac{1}{2} < \eta^2 > \delta t$.

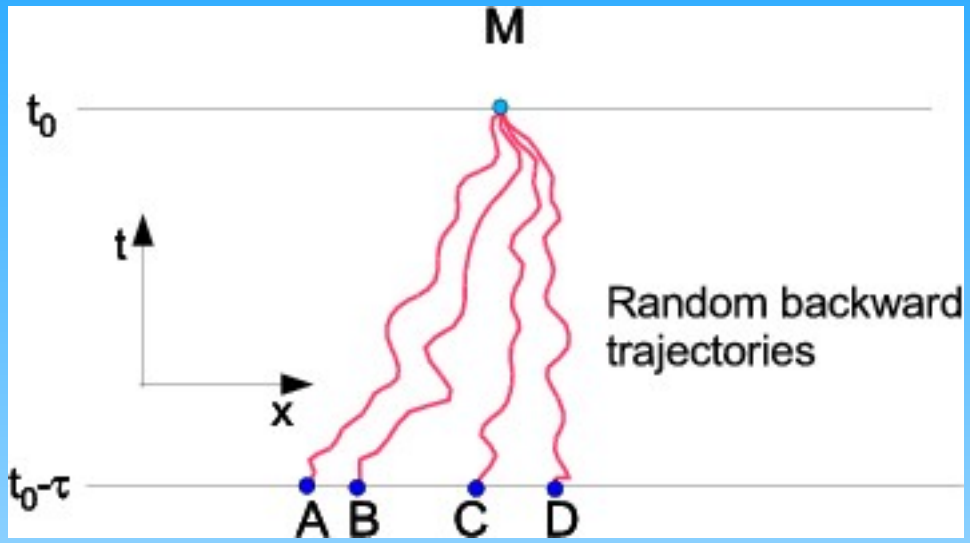

How to estimate Lagrangian diffusivity?

Pure advection (no diffusion) generates a number of spurious laminae which are not observed in the tracer profiles.

D can be estimated by adjusting diffusion until the reconstructed transect exhibits the same *roughness* as the observed transect r when well identified structures are similar.

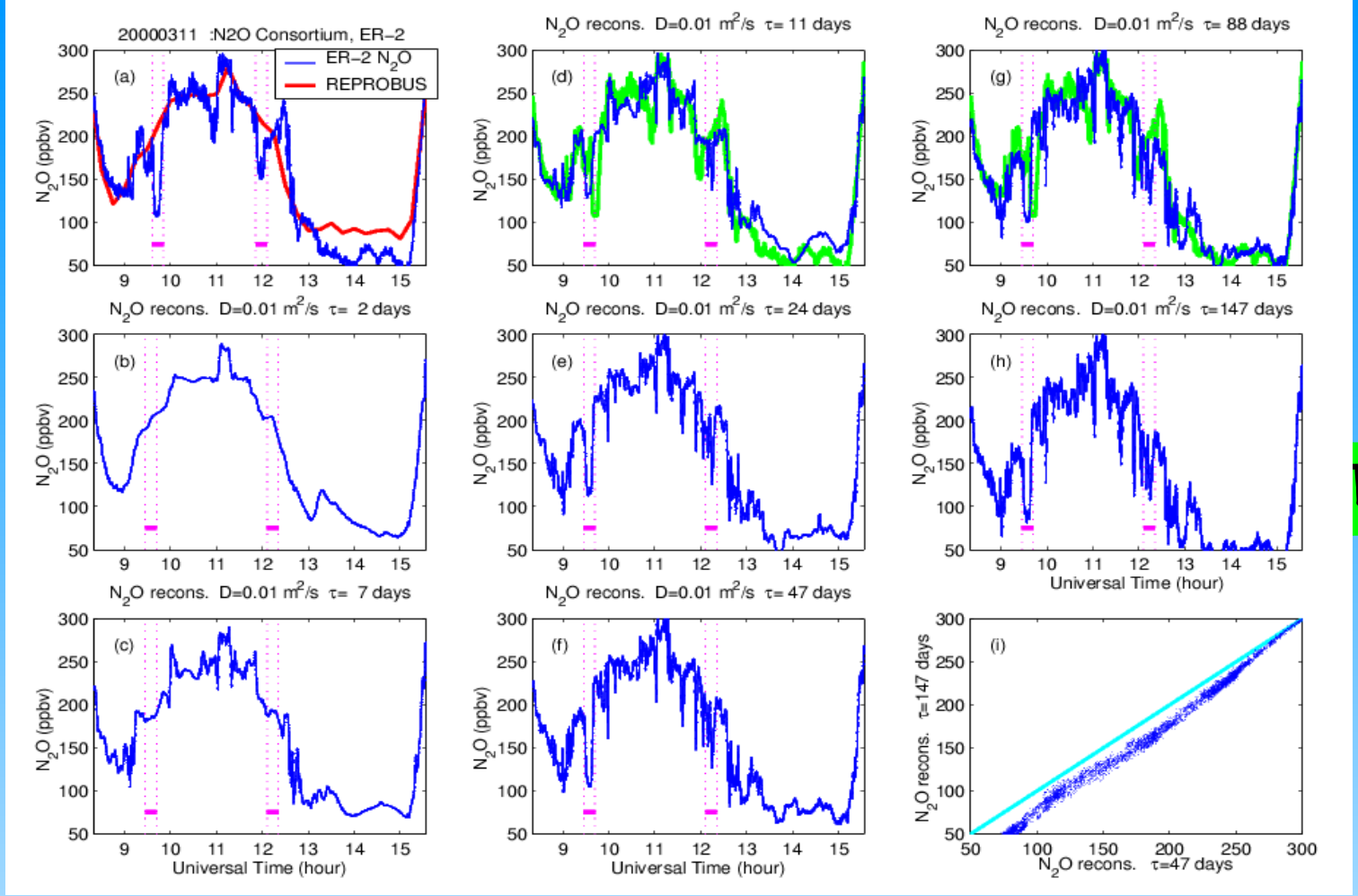

Tracer N_2O

Convergence of diffusive reconstructions

Reactive O_3

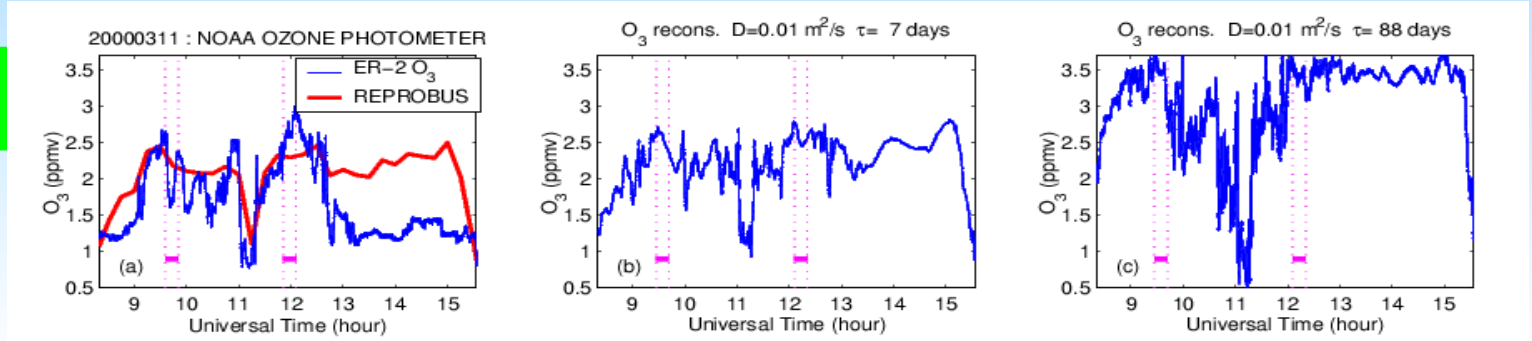

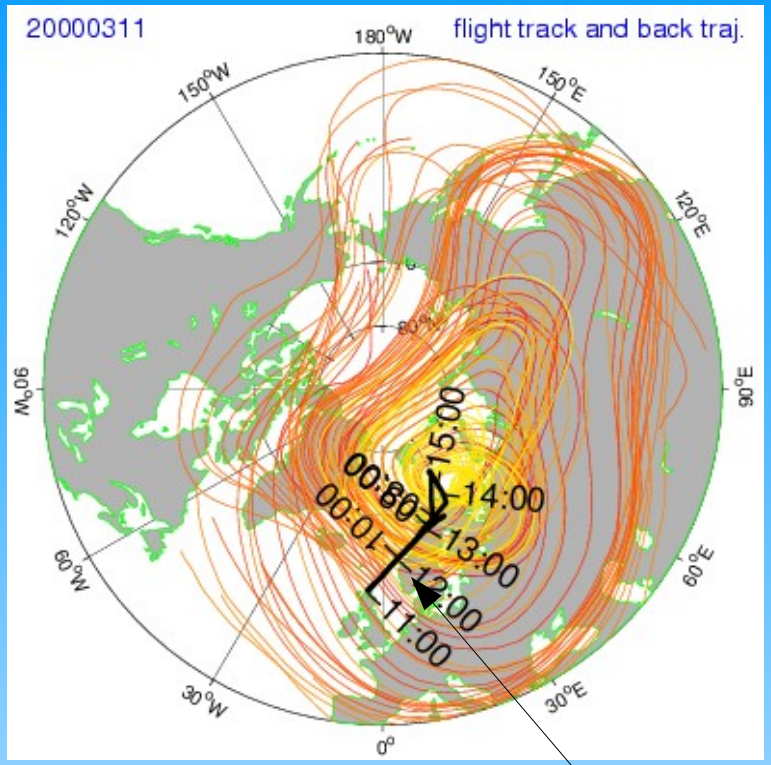

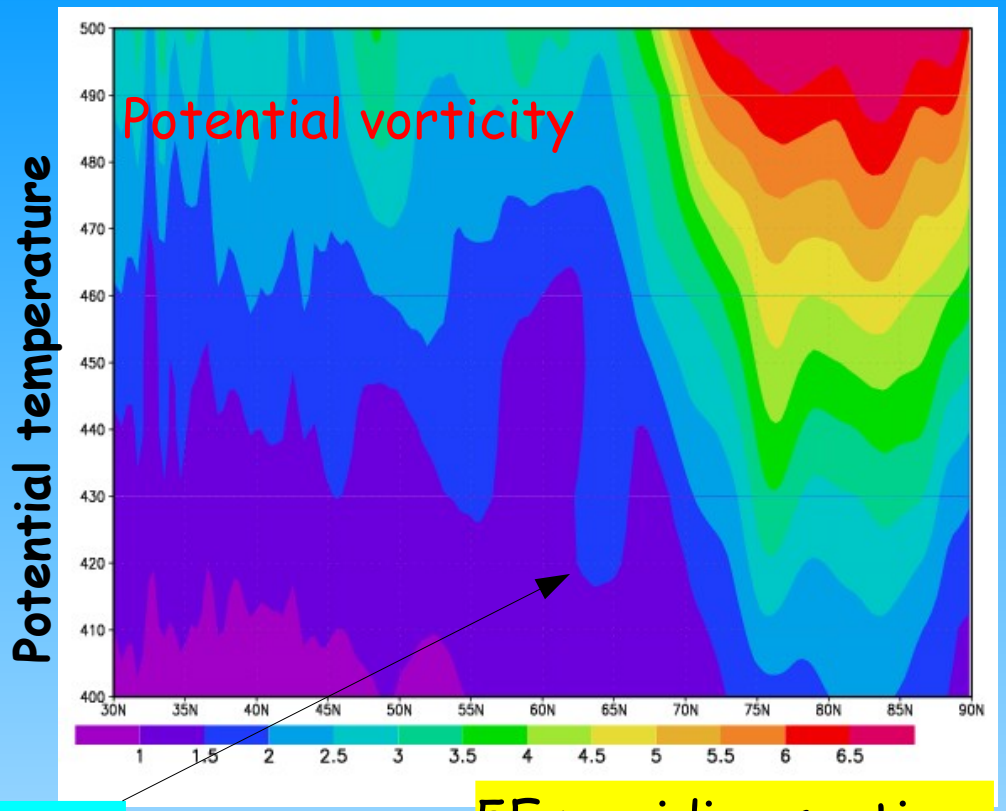

5E meridian section

filament

Filament encounter on 3 March 2000

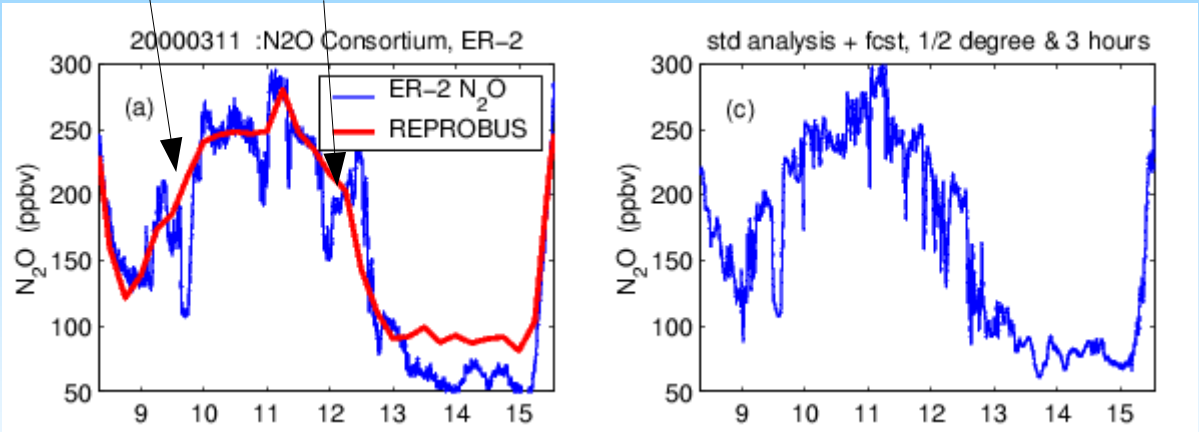

Local variations of Lagrangian turbulent diffusion

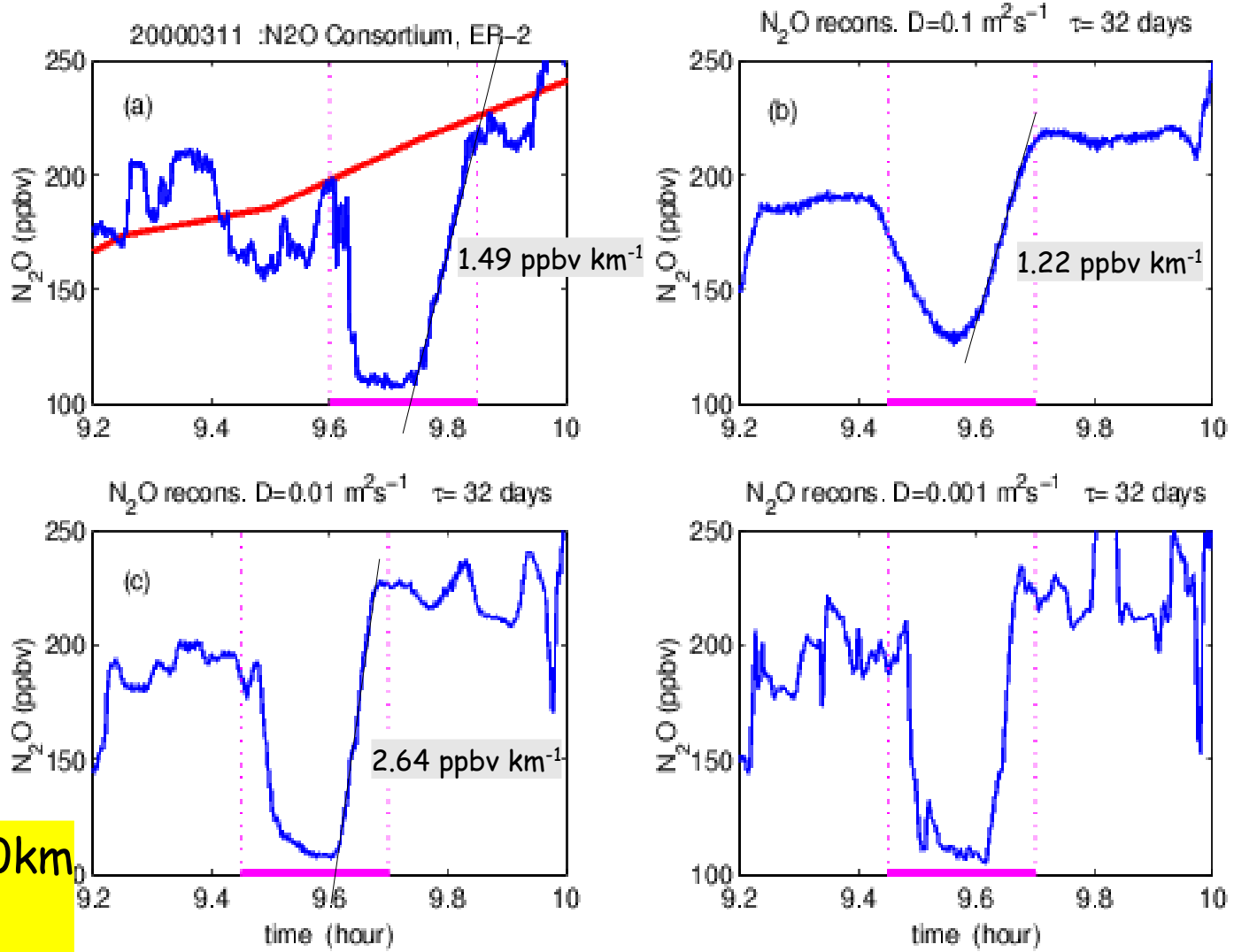

Filament width 100km
right edge 36 km
left edge 2.5 km

Intermediate Summary

Basic facts about transport and mixing in the lower stratosphere

- Quasi-layerwise motion generates a large amount of small-scale sheets by advection seen as filaments in 2D maps and laminae in profiles or transects .
- Advection is dominated by structures in the wind field that are of sufficiently large scale to be resolved by operational analysis $\Rightarrow$ chaotic folding and stretching
- Laminae in the tracers are observed by in situ instruments at scales unresolved by NWP models.
- Sheets are sloping with an aspect ratio determined by the ratio between vertical shear and horizontal strain, $\approx$ 250 (Haynes & Anglade, 1997) in the lower stratosphere (1 km in the horizontal $\Leftrightarrow$ 4 m in the vertical). As a result aircraft measurements have generally much higher equivalent resolution than balloon soundings.
- Sheet thickness is bounded by 3D unresolved turbulence that is primarily acting as vertical mixing.

Transport et mélange

I Introduction et exemples

II Eléments de théorie

III Reconstructions des champs de traceurs

IV Barrières de transport

V Diagrammmes traceur-traceur et lignes de mélange

V Un exemple de méthode semi-lagrangienne

DYNAMICAL BARRIERS

Aircraft section across the edge of the Antarctic polar vortex at an altitude of about 18 km

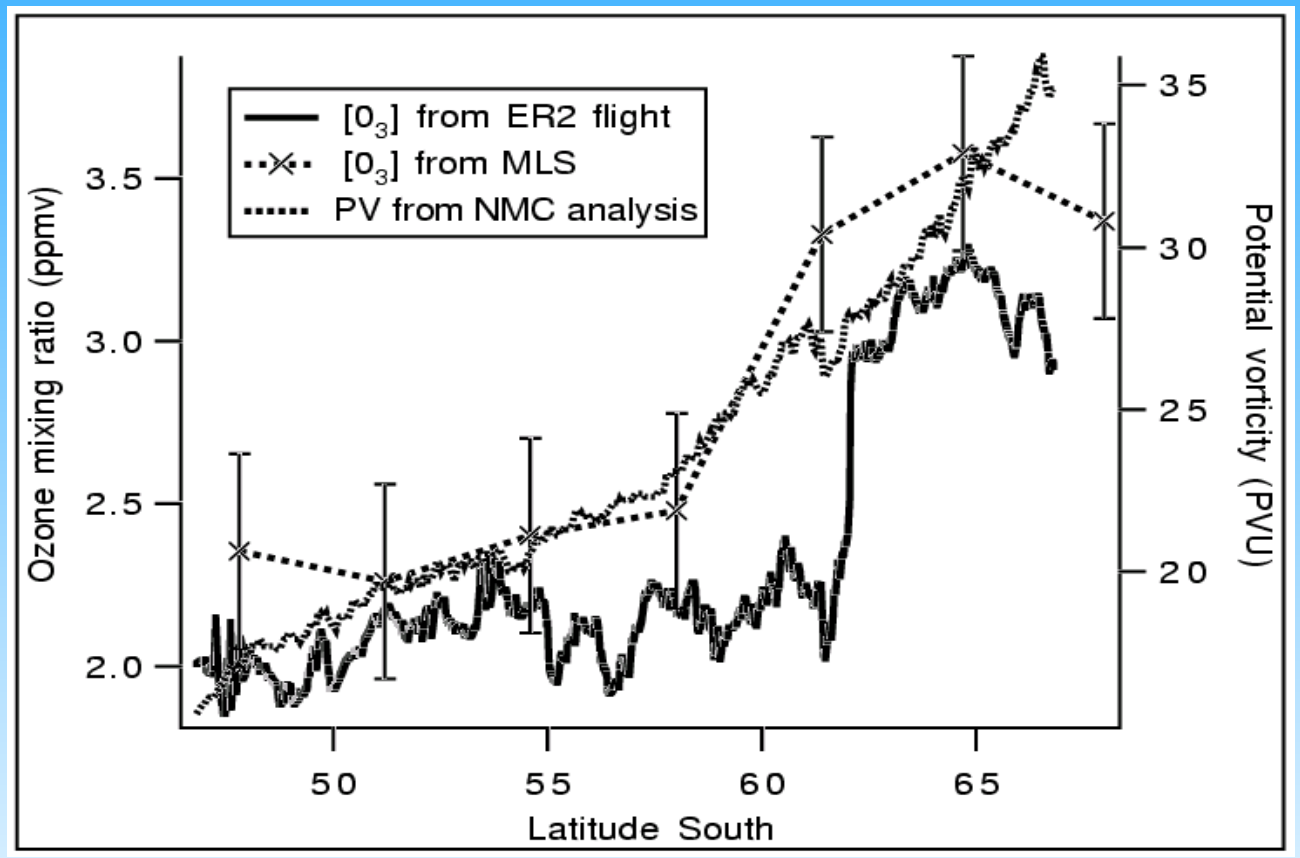

Dynamical barriers are required to explain large PV or tracer gradients

Erosion d'un vortex soumis à un cisaillement externe
Generation de filaments et de gradients à la périphérie

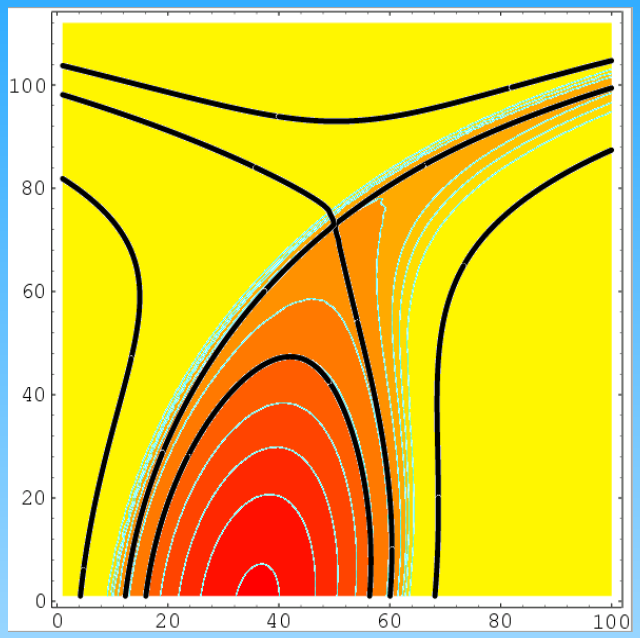

Carte de fonction de courant et vorticité (la vorticité peut être remplacée par un traceur).
Cas d'érosion lente.

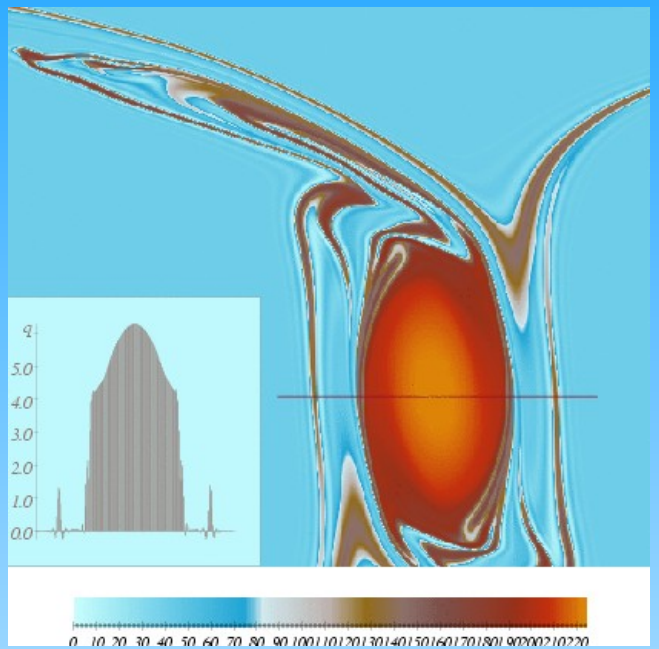

Carte de vorticité et section le long de la ligne transverse.
Cas de l'érosion rapide.

Carte du vortex polaire Antarctique. PV et lignes d'étirement (Lyapunov) maximums (backward et forward).

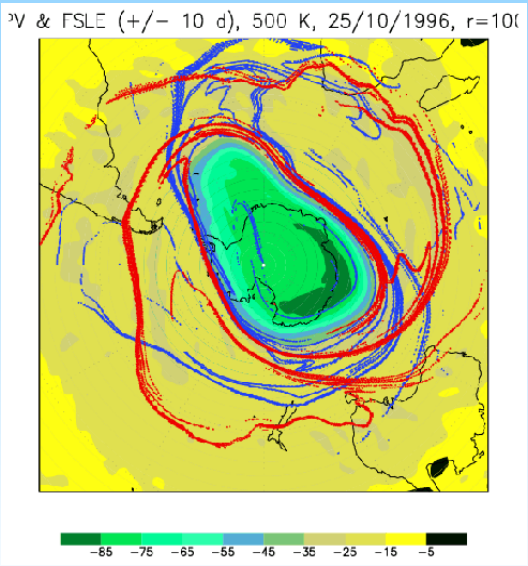

Intersection of stable and unstable material lines: hyperbolic trajectories

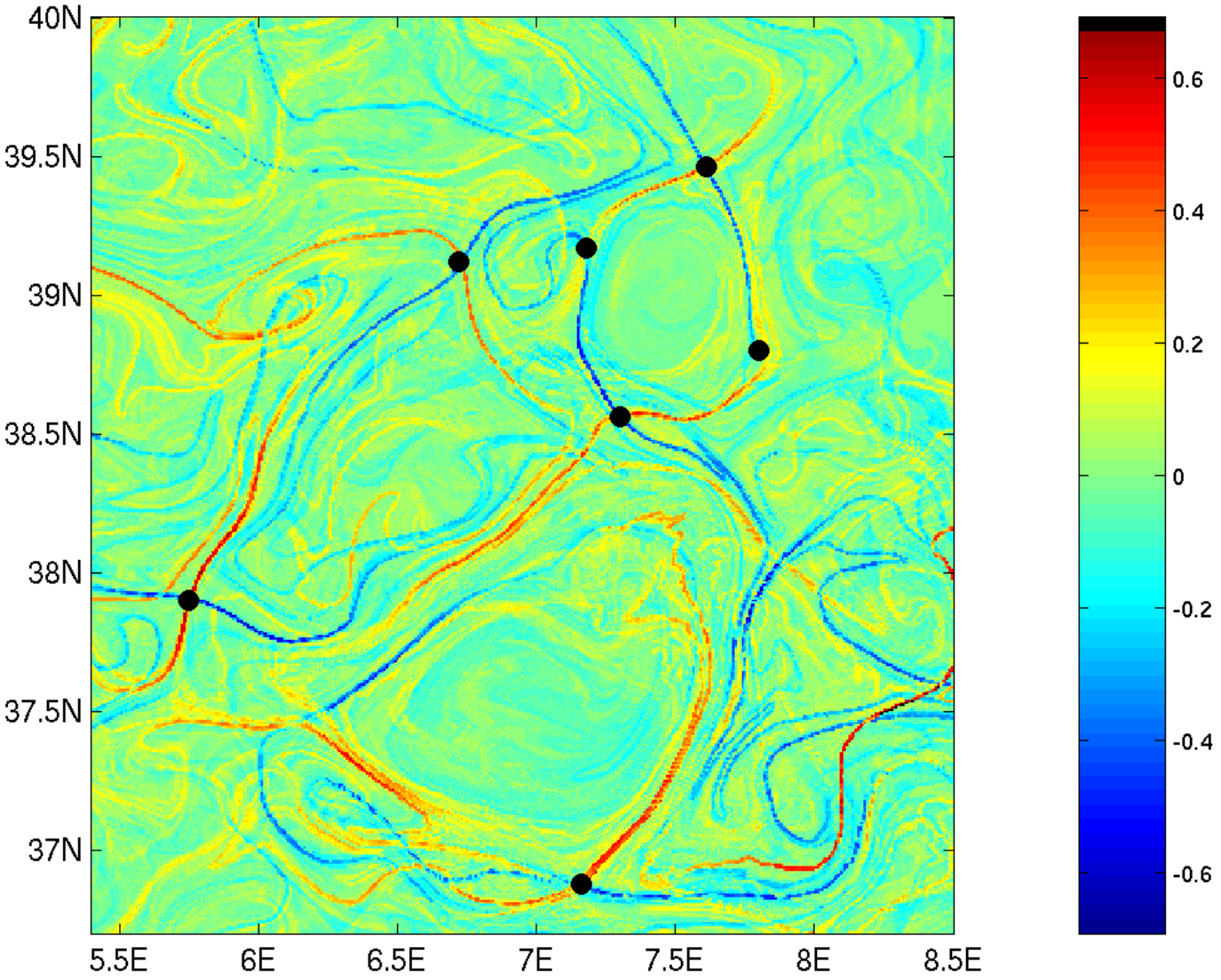

day 1

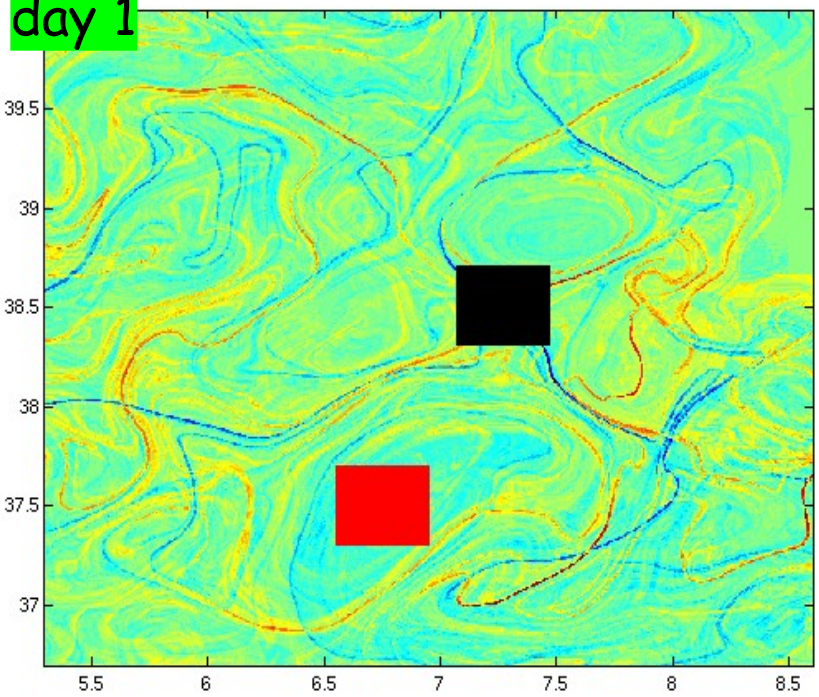

day 2

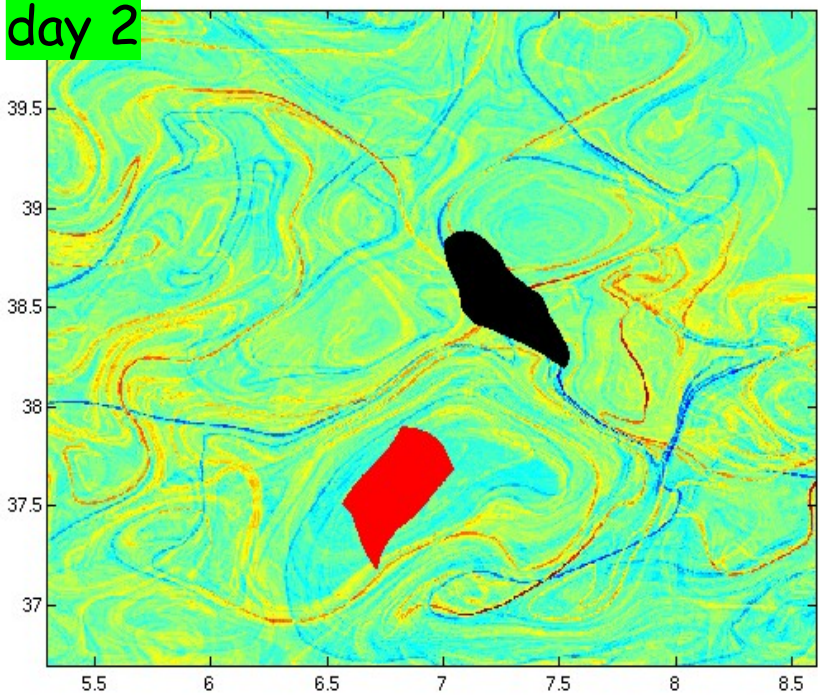

day 3

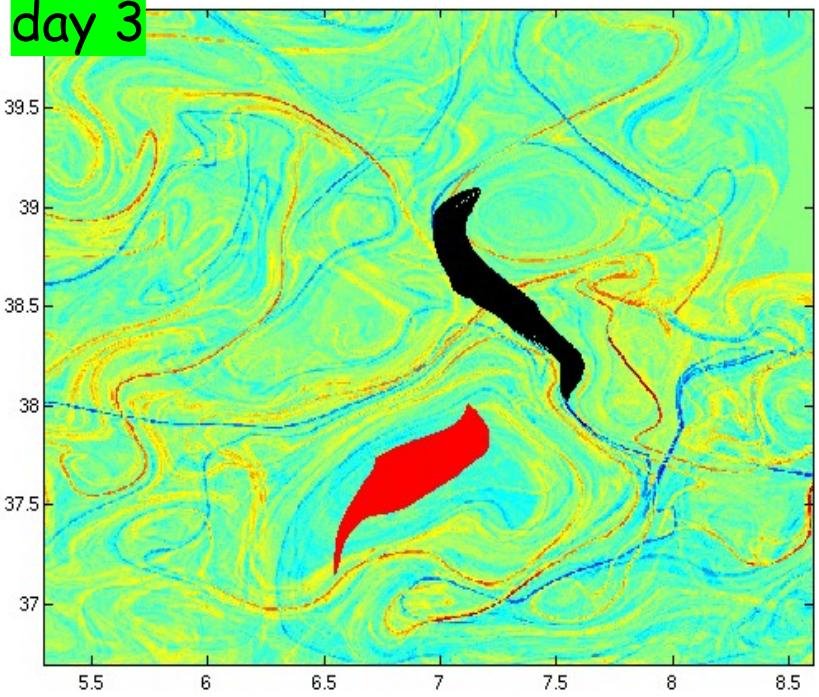

day 5

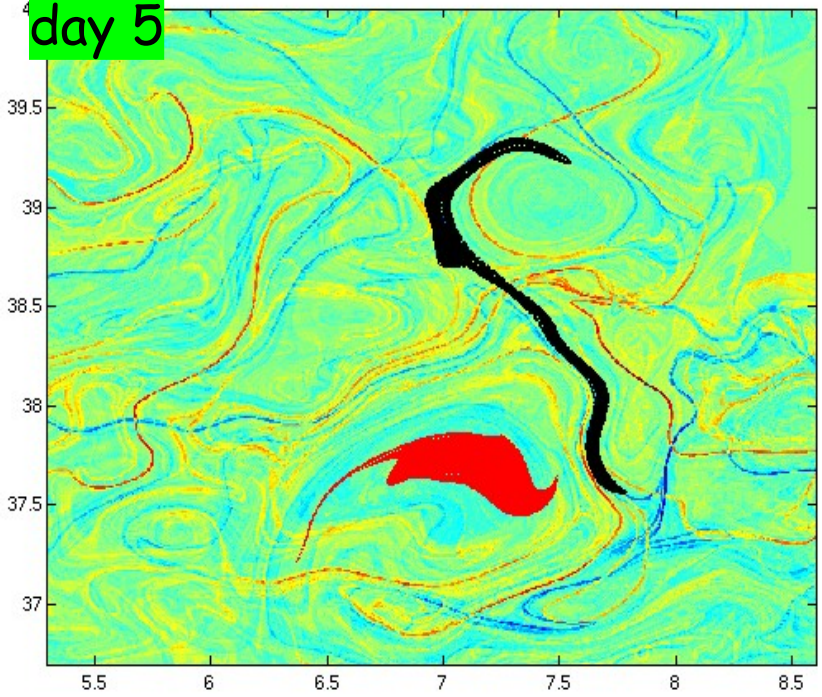

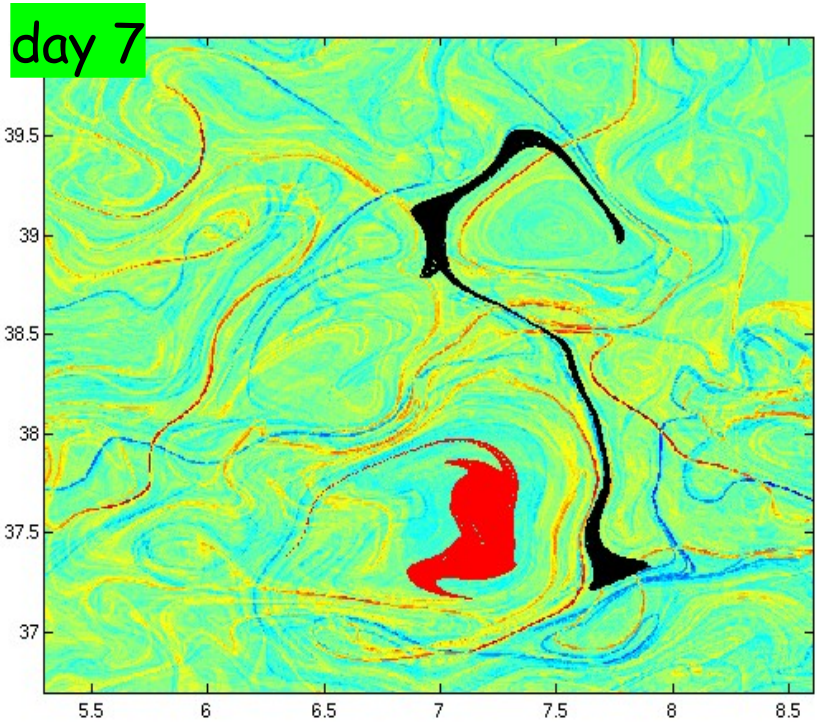
day 7
39.5
39
38.5
38
37.5
37
5.5
6
6.5
7
7.5
8
8.5

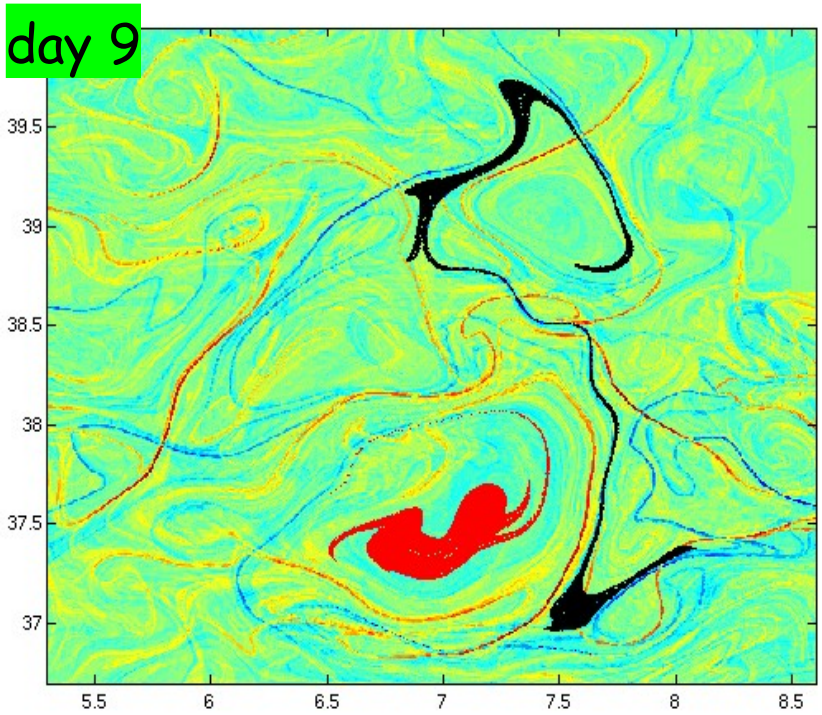
day 9
39.5
39
38.5
38
37.5
37
5.5
6
6.5
7
7.5
8
8.5

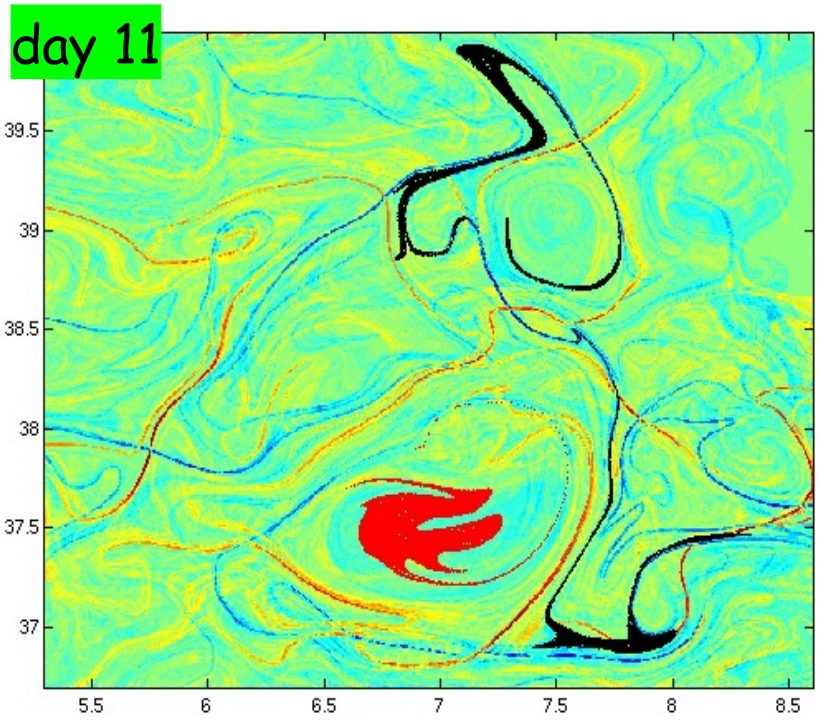
day 11
39.5
39
38.5
38
37.5
37
5.5
6
6.5
7
7.5
8
8.5

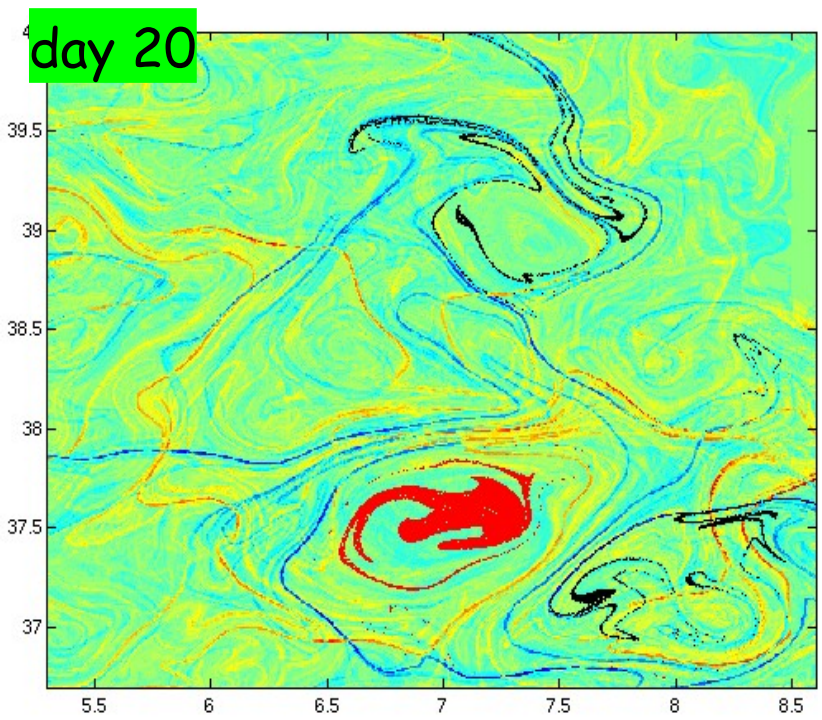
day 20
39.5
39
38.5
38
37.5
37
5.5
6
6.5
7
7.5
8
8.5

Effective diffusivity in practice

$$K_{\mathrm{eff}}(A,t) = \frac{\partial A}{\partial C} \oint_{\gamma(C,t)} \kappa |\nabla c|\, dl = \frac{\langle \kappa |\nabla c|^2 \rangle}{(\partial C/\partial A)^2}$$

- Keff (Leq) is well defined from contour averaging on isentropic surfaces
- Measures mixing as the amount of foldings beared by a given contour.
- Pro: Is a diffusivity. Easily calculated. Depends weakly on the quantity being contoured. Usable as a turbulent parameterization in 2D vert-lat models.
- Con: Limited to isentropic motion. Does not diagnose variation of diffusion along contours.

L_{eq} as a function of log-pressure height and ϕ_e.

Increased mixing in the summer lower stratosphere

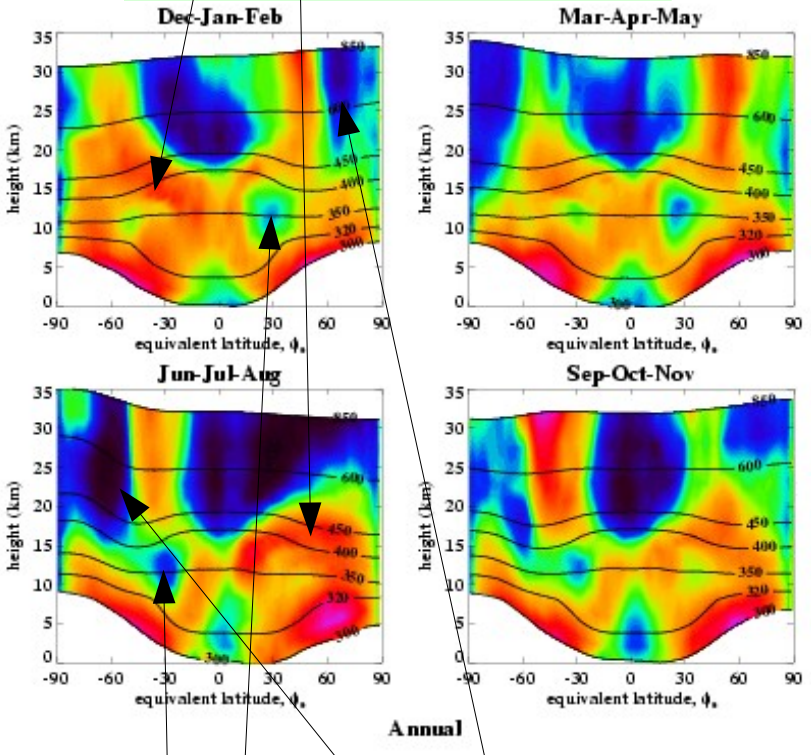

see Haynes and Shuckburgh, 2000, JGR, 105, 22777-22810.

Subtropical jets and polar vortex jets as minima (barriers) in effective diffusivity

Transport et mélange

I Introduction et exemples

II Eléments de théorie

III Reconstructions des champs de traceurs

IV Barrières de transport

V Diagrammmes traceur-traceur et lignes de mélange

V Un exemple de méthode semi-lagrangienne

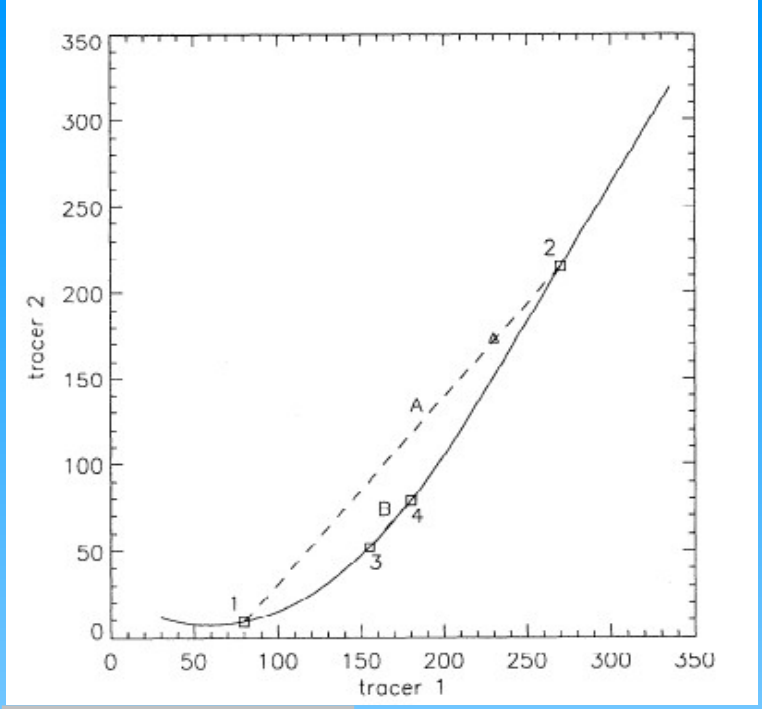

Waugh et al., JGR, 102, p13119, 1997

In well-mixed stratified regions, tracers tend to form a compact relation (indexed, e.g., by the potential temperature).
A sudden mixing event between two different layers generate a mixing line which can be identified as such from data if the relation is non linear.

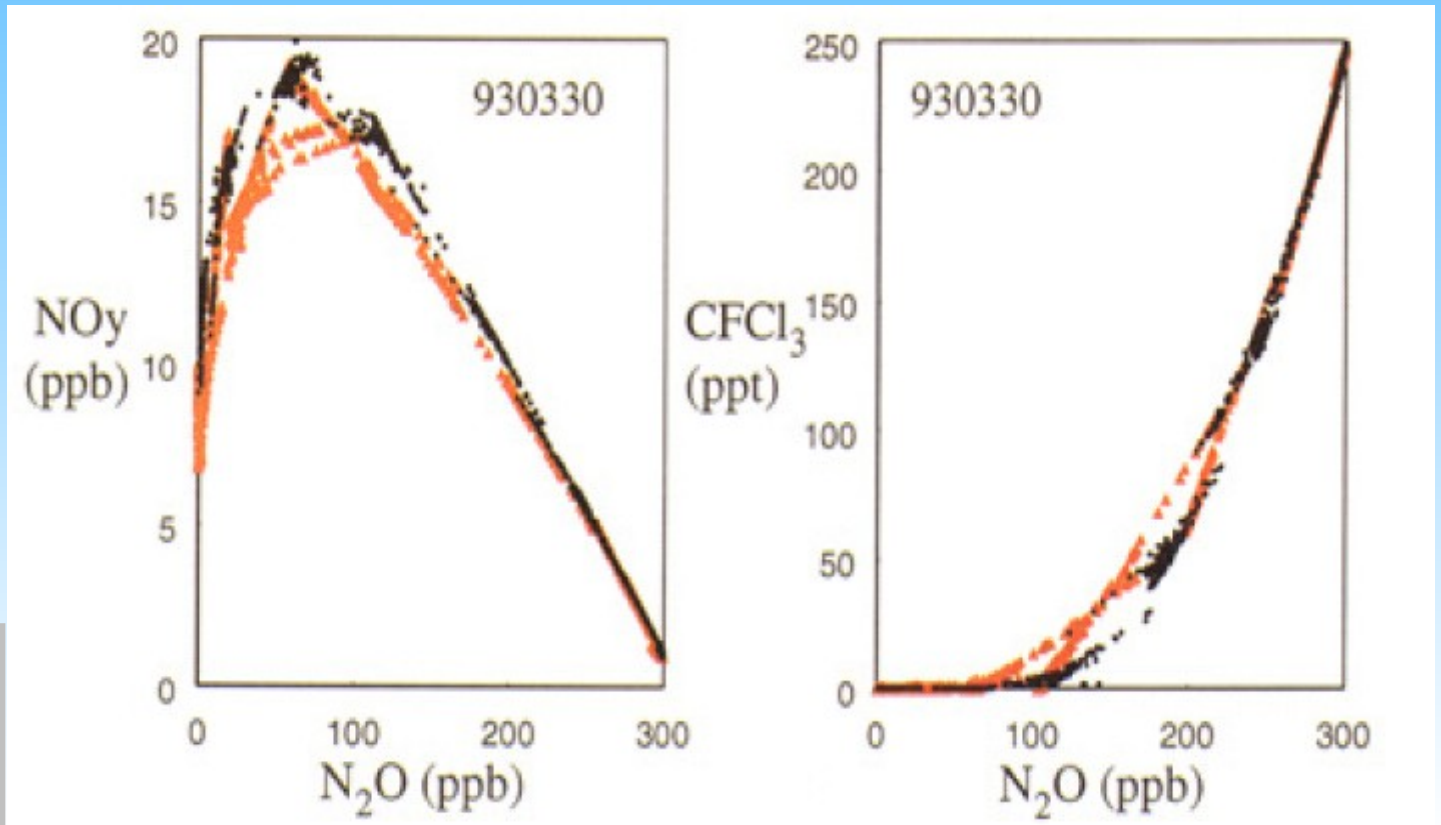

Plumb et al., JGR, 105, p10047, 2000.

Barrière de mélange à la tropopause

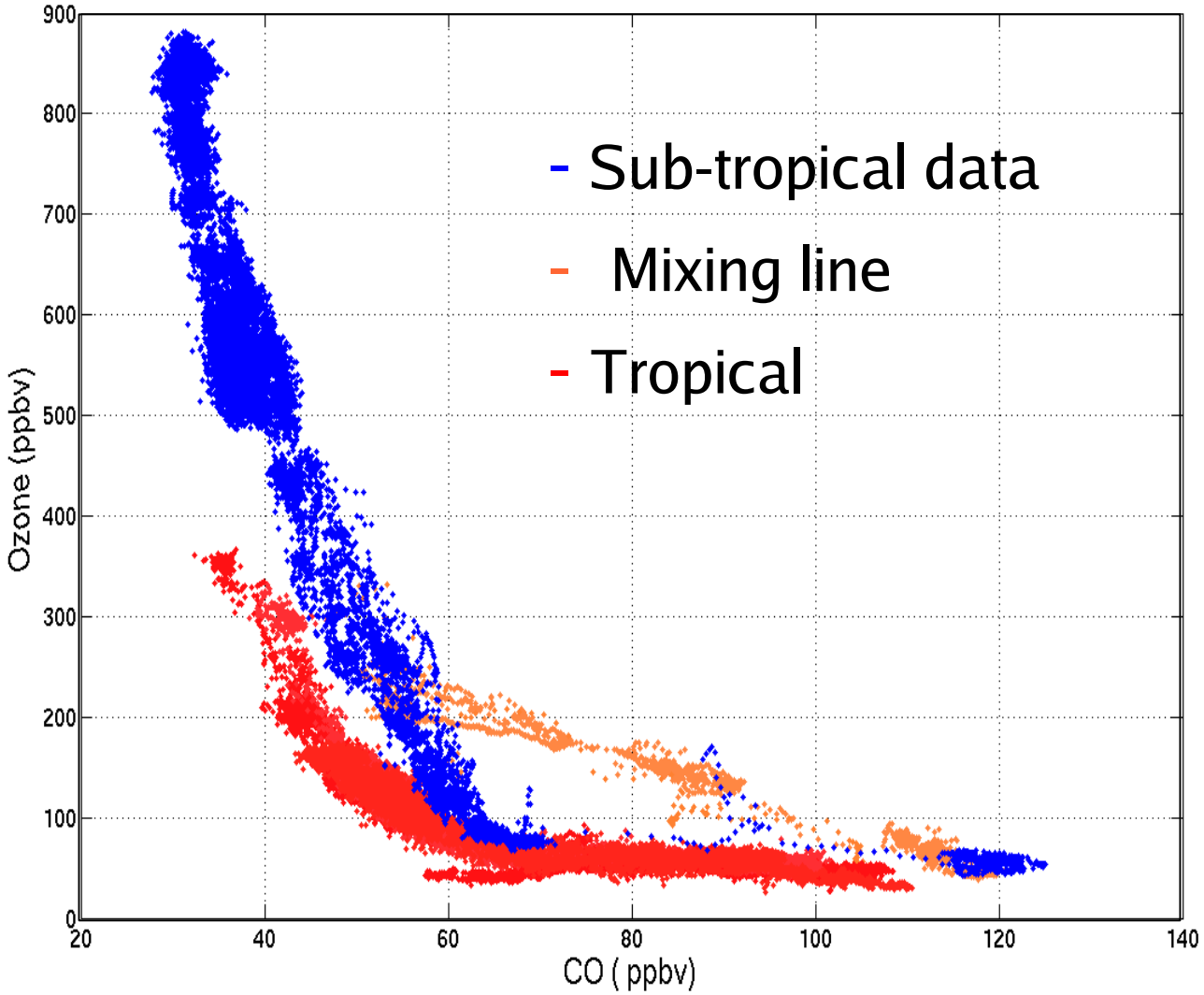

James et Legras, ACP, 2008

Numerical methods of transport for chemical species

The numerical problem for advection-diffusion is linear in the tracer variables, that is a priori simpler than the full Navier-Stokes equation.
However, some constrains (positivity, mass coservation, monotonicity, ...) are highly desirable.

Spectral and standard finite-difference methods are easily available and very accurate for transport but induce bad side effects like loss of mass conservation and non posivity. Largely abandonned for tracers.

Very popular schemes are finite-volume methods (upwind or more sophisticated versions (Prather, Muscl). See VanLeer, 1977, J. Comput. Phys., 23, p276. Such scheme exhibit numerical diffusion that depends on the velocity, not on his gradient.

Semi-Lagrangian or Lagrangian schemes based on deformable grids and renoding.

Transport et mélange

I Introduction et exemples

II Eléments de théorie

III Reconstructions des champs de traceurs

IV Barrières de transport

V Diagrammmes traceur-traceur et lignes de mélange

V Un exemple de méthode semi-lagrangienne

CLAMS numerical advection scheme

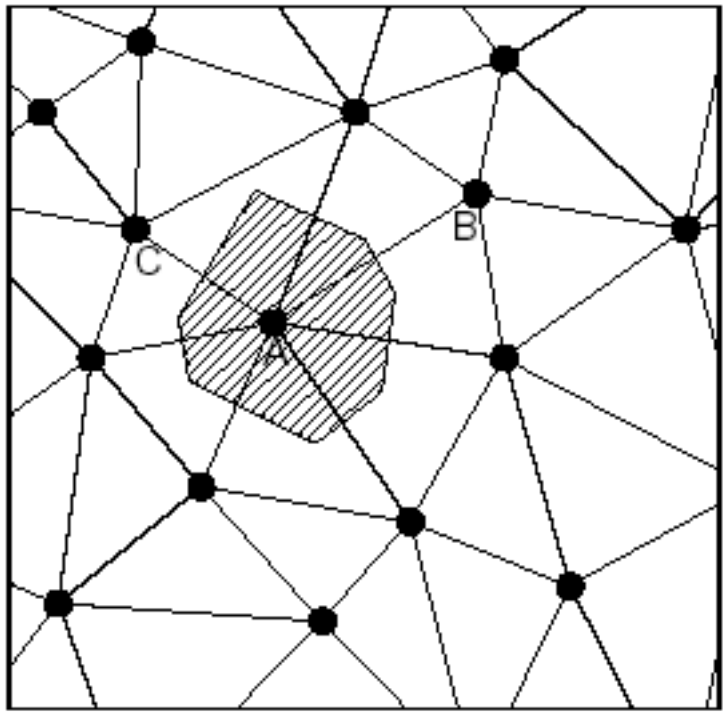

quasiuniform distribution
of air parcels
Delaunay triangulation ⇒
next neighbors

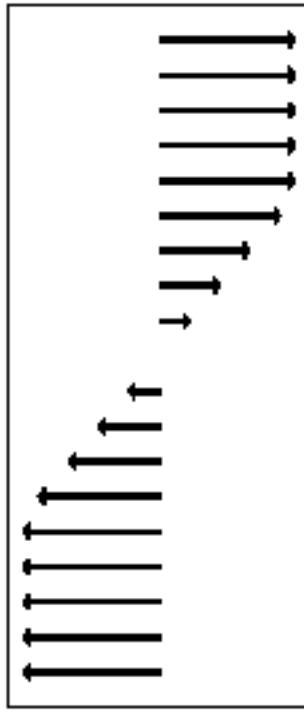

sheared flow
$\Delta t = 6 - 24$
hours

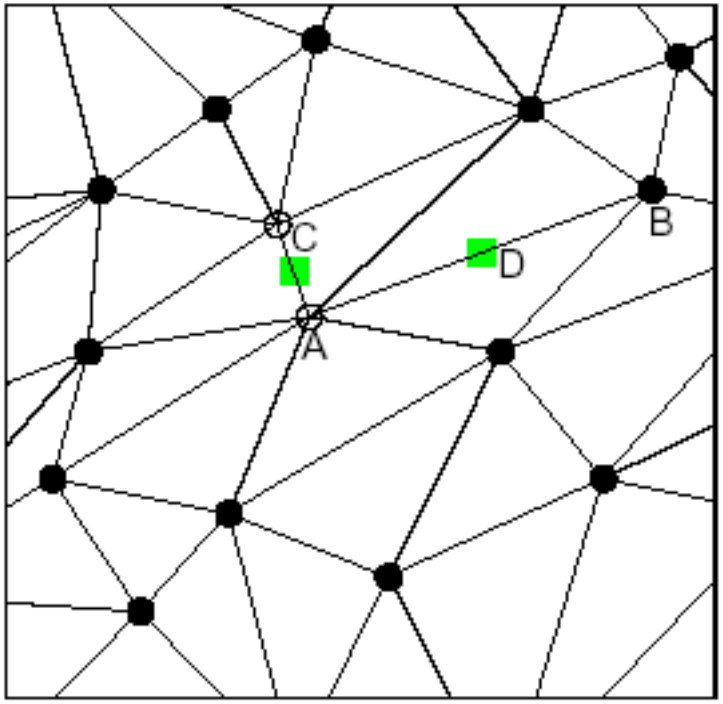

grid adaptation =
regridding of the deformed grid
⇒ new air parcels
⇒ interpolations (num. diffusion)
⇒ mixing

Mc Kenna et al., 2002, JGR, 107, 2000JD000114;
Konopka et al., 2004, JGR, 109, 2003JD003792

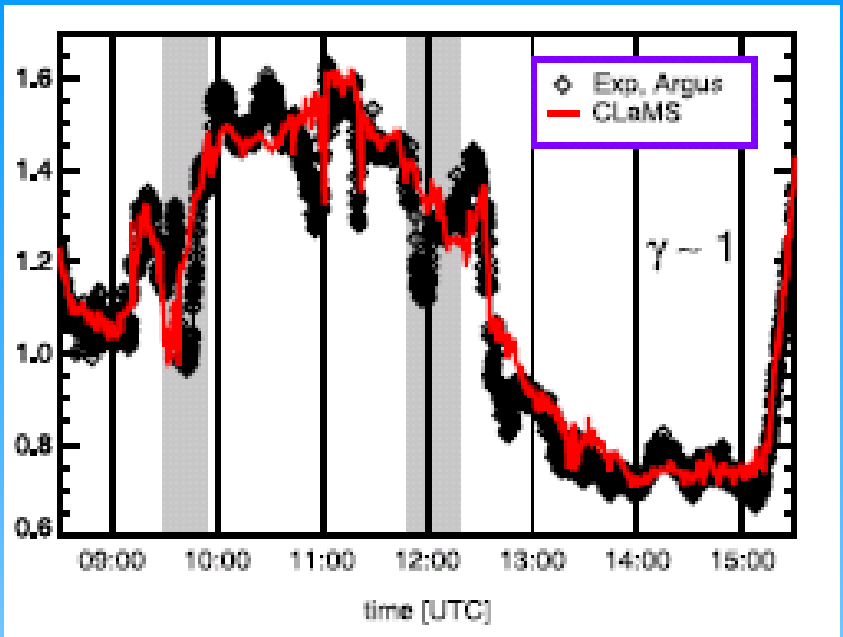

CLAMS results
for SOLVE campaign

Argus CH4 versus
CLAMS

Konopka et al., 2004,
JGR, 109,
2003JD003792

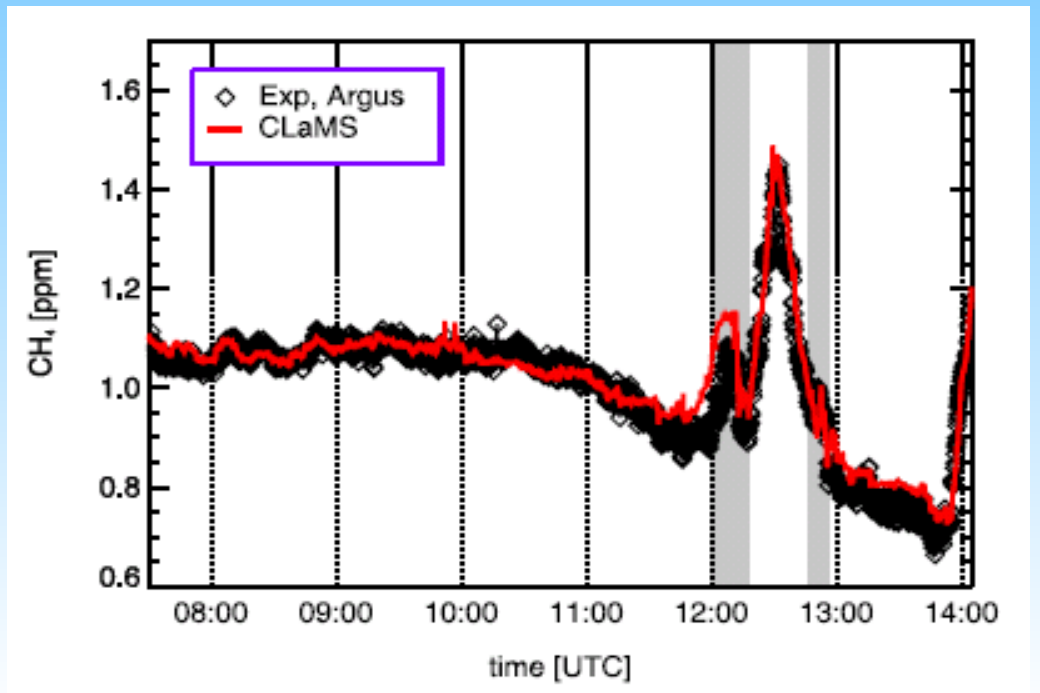

Transport et mélange

I Introduction et exemples

II Eléments de théorie

III Reconstructions des champs de traceurs

IV Barrières de transport

V Diagrammmes traceur-traceur et lignes de mélange

V Un exemple de méthode semi-lagrangienne

VI Echanges à la tropopause

Transport vertical dans un cyclone extratropical

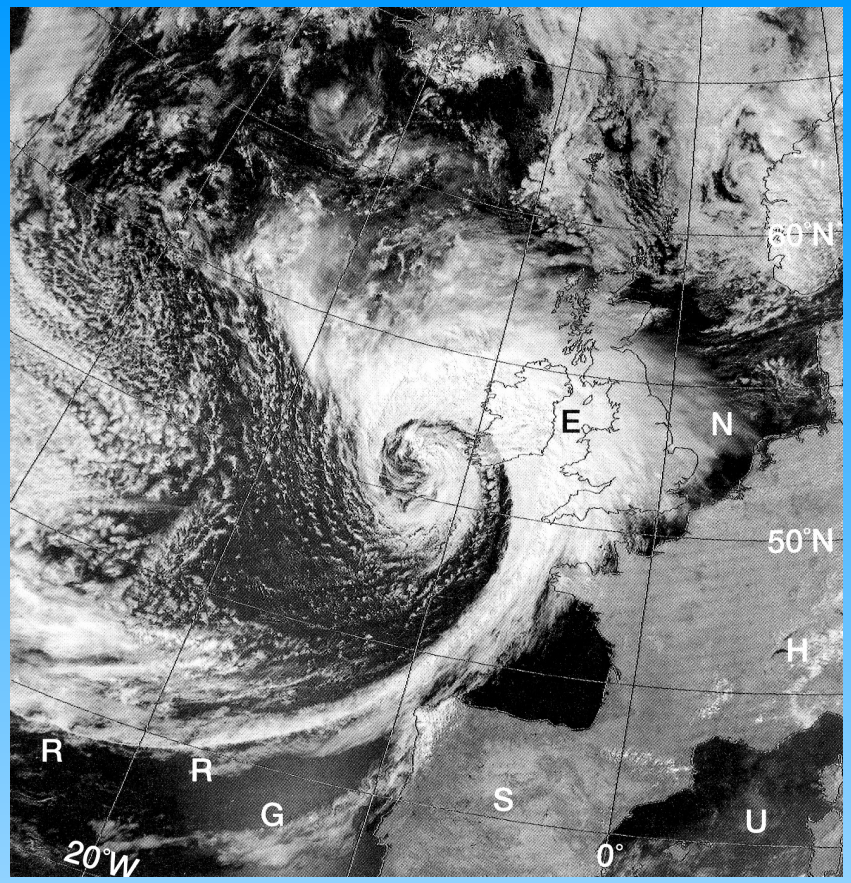

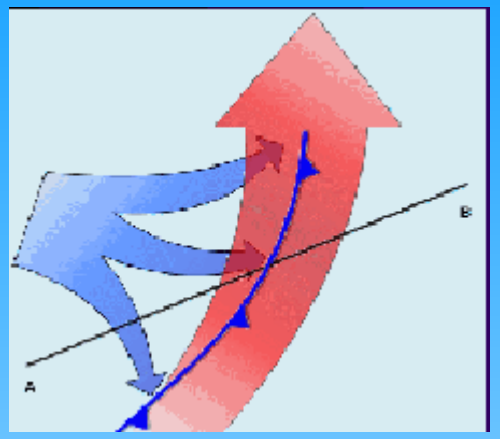

Warm conveyor belt

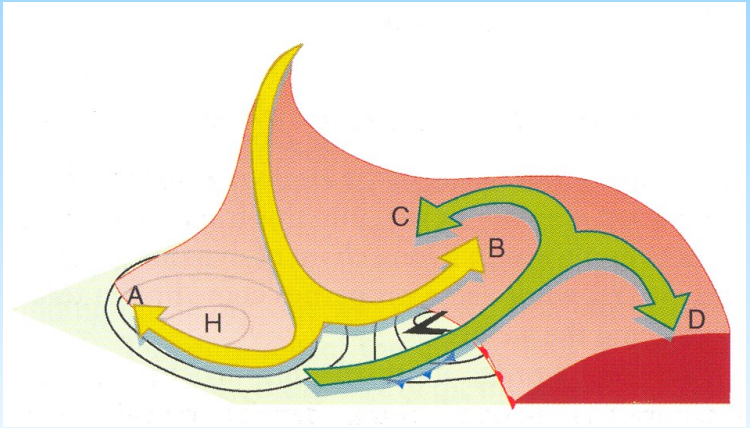

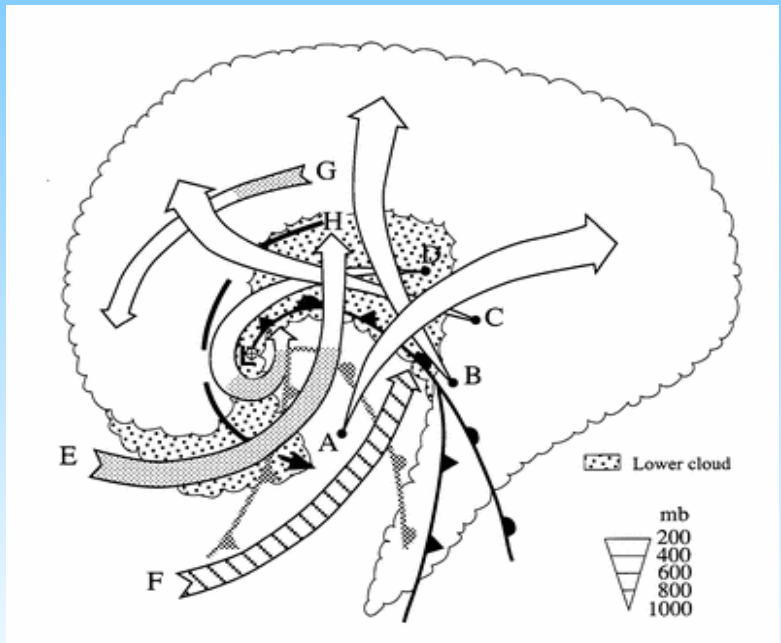

Occlusion

An example of a WCB reaching into the LS

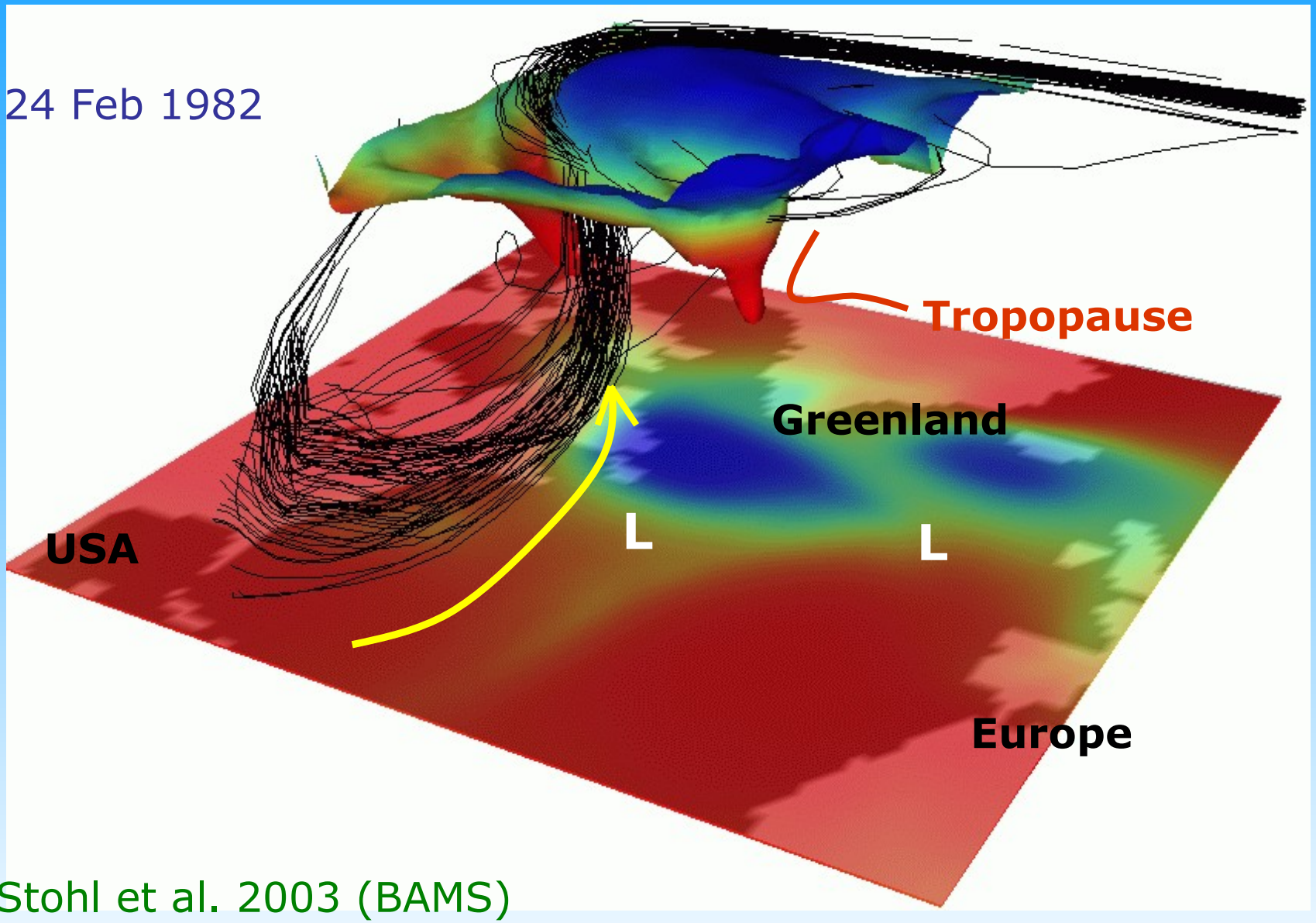

Stohl et al. 2003 (BAMS)

The Brewer Dobson meridional circulation

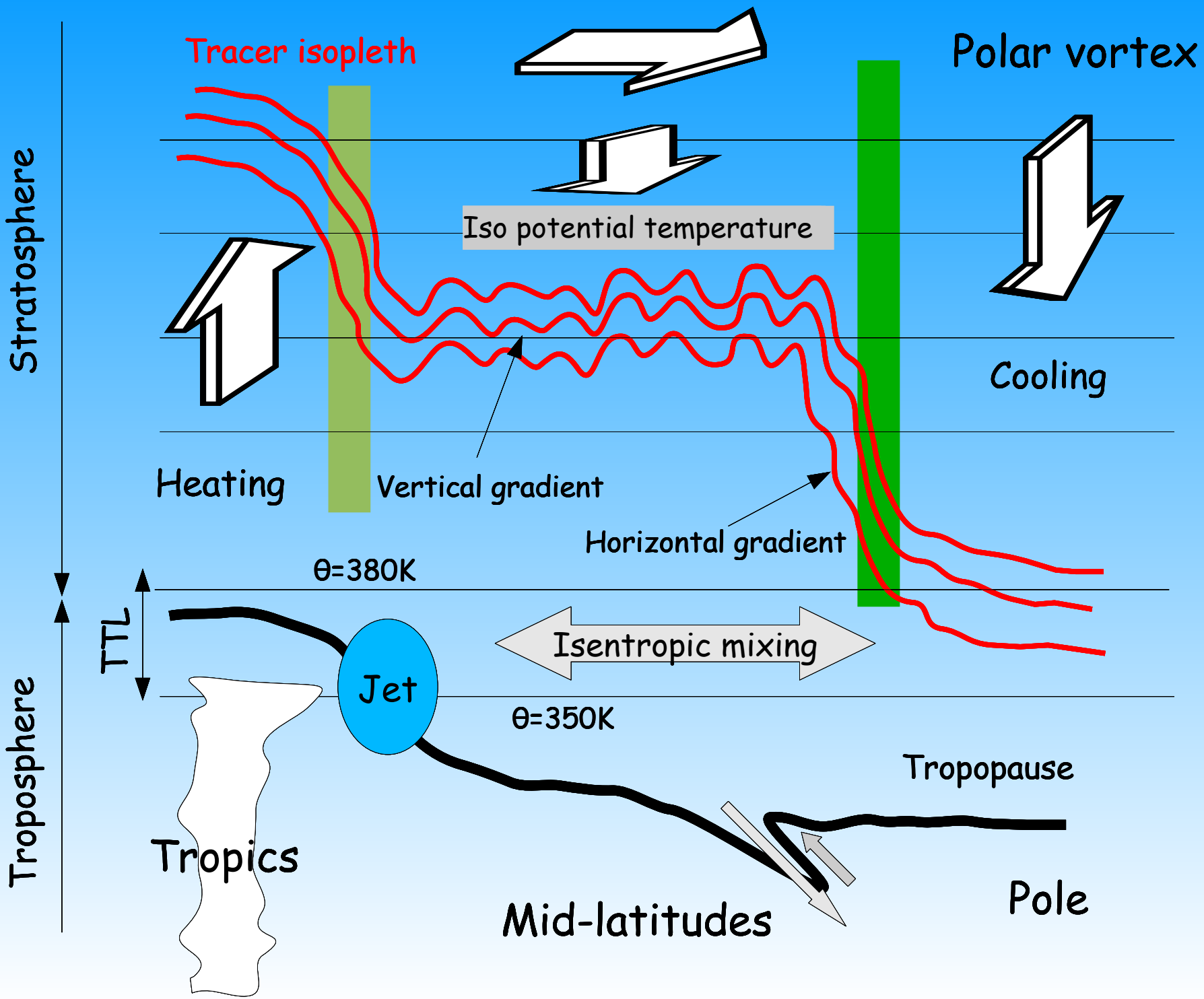

Circulation verticale dans les tropiques et convection

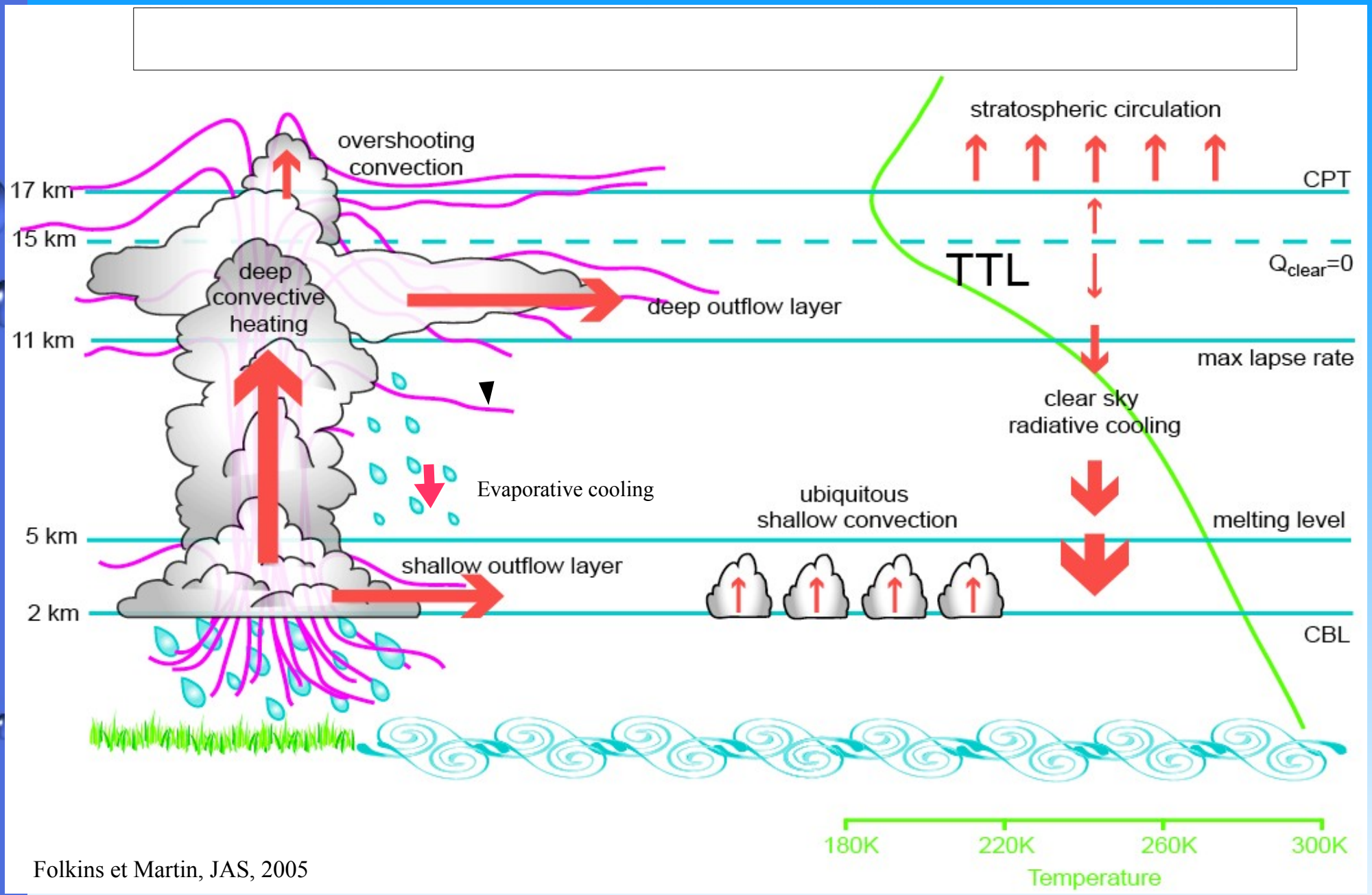

Folkins et Martin, JAS, 2005